Derksen RH, de Groot PG. β2-Glycoprotein I is proteolytically cleaved in vivo upon activation of fibrinolysis. Thromb Haemost. 1999;81:87-95.

23. Itoh Y, Inuzuka K, Kohno I, et al. Highly increased plasma concentrations of the nicked form of β2-glycoprotein I in patients with leukemia and with lupus anticoagulant: measurement with a monoclonal antibody specific for a nicked form of domain V. J Biochem (Tokyo). 2000;128:1017-1024.
24. Igarashi M, Matsuura E, Igarashi Y, et al. Human β2-glycoprotein I as an anticardiolipin cofactor determined using deleted mutants expressed by a Baculovirus system. Blood. 1996;87:3262-3270.
25. Matsuura E, Igarashi Y, Fujimoto M, et al. Heterogeneity of anticardiolipin antibodies defined by the anticardiolipin cofactor. J Immunol. 1992;148:3885-3891.
26. Matsuura E, Inagaki J, Kasahara H, et al. Proteolytic cleavage of β2-glycoprotein I: reduction of antigenicity and the structural relationship. Int Immunol. 2000;12:1183-1192.
27. Ranby M, Wallen P. A sensitive parabolic rate assay for tissue plasminogen activator. In: Davidson JF, Nilson IM, Asted B, eds. Progress in Fibrinolysis. Vol 5. New York, NY: Churchill Livingstone; 1981:232-235.
28. Bouma B, de Groot PG, van den Elsen JM, et al. Adhesion mechanism of human β2-glycoprotein I to phospholipids based on its crystal structure. EMBO J. 1999;18:5166-5174.
29. Schwarzenbacher R, Zeth K, Diederichs K, et al. Crystal structure of human β2-glycoprotein I: implications for phospholipid binding and the antiphospholipid syndrome. EMBO J. 1999;18:6228-6239.
30. Hoshino M, Hagihara Y, Nishii I, Yamazaki T, Kato H, Goto Y. Identification of the phospholipid-binding site of human β2-glycoprotein I domain V by heteronuclear magnetic resonance. J Mol Biol. 2000;304:927-939.
31. Lucas MA, Fretto LJ, McKee PA. The binding of human plasminogen to fibrin and fibrinogen. J Biol Chem. 1983;258:4249-4256.
32. Wu HL, Chang BI, Wu DH, et al. Interaction of plasminogen and fibrin in plasminogen activation. J Biol Chem. 1990; 265:19658-19664.
33. Christensen U. C-terminal lysine residues of fibrinogen fragments essential for binding to plasminogen. FEBS Lett. 1985;182:43-46.
34. Tran-Thang C, Kruithof EK, Atkinson J, Bachmann F. High-affinity binding sites for human Glu-plasminogen unveiled by limited plasmic degradation of human fibrin. Eur J Biochem. 1986;160:599-604.
35. Matsuka YV, Novokhatny VV, Kudinov SA. Fluorescence spectroscopic analysis of ligand binding to kringle 1 + 2 + 3 and kringle 1 fragments from human plasminogen. Eur J Biochem. 1990;190:93-97.
36. Chang Y, Mochalkin I, McCance SG, Cheng B, Tulinsky A, Castellino FJ. Structure and ligand binding determinants of the recombinant kringle 5 domain of human plasminogen. Biochemistry. 1998;37:3258-3271.
37. Collen D, Lijnen HR. Basic and clinical aspects of fibrinolysis and thrombolysis. Blood. 1991;78:3114-3124.
38. Thorsen S, Clemmensen I, Sottrup-Jensen L, Magnusson S. Adsorption to fibrin of native fragments of known primary structure from human plasminogen. Biochem Biophys Acta. 1981;668:377-387.

Clin Exp Immunol 2004; 136:585–590 doi:10.1111/j.1365-2249.2004.02477.x

Anti-mannose binding lectin antibodies in sera of Japanese patients with systemic lupus erythematosus

R. TAKAHASHI*, A. TSUTSUMI*, K. OHTANI†, D. GOTO*, I. MATSUMOTO*, S. ITO*, N. WAKAMIYA† & T. SUMIDA*
*Division of Rheumatology, Department of Internal Medicine, Institute of Clinical Medicine, University of Tsukuba, Tsukuba-city and †Department of Microbiology, Asahikawa Medical College, Asahikawa-city, Japan

(Accepted for publication 16 March 2004)

SUMMARY

Mannose-binding lectin (MBL) is a key element in innate immunity with functions and structure similar to that of complement C1q. It has been reported that MBL deficiency is associated with occurrence of systemic lupus erythematosus (SLE). We hypothesized that anti-MBL antibodies, if present, would affect the occurrence or disease course of SLE, by reduction of serum MBL levels, interference of MBL functions, or binding to MBL deposited on various tissues. To address this hypothesis, we measured the concentration of anti-MBL antibodies in sera of 111 Japanese SLE patients and 113 healthy volunteers by enzyme immunoassay. The titres of anti-MBL antibodies in SLE patients were significantly higher than those in healthy controls. When the mean + 2 standard deviations of controls was set as the cut off point, individuals with titres of anti-MBL antibodies above this level were significantly more frequent in SLE patients (9 patients) than in controls (2 persons). One SLE patient had an extremely high titre of this antibody. No associations of titres of anti-MBL antibodies and (i) genotypes of MBL gene, (ii) concentrations of serum MBL, or (iii) disease characteristics of SLE, were apparent. Thus, we have confirmed that anti-MBL antibodies are indeed present in sera of some patients with SLE, but the significance of these autoantibodies in the pathogenesis of SLE remains unclear.

Keywords Lupus/ systemic lupus erythematosus autoantibodies MBL C1q polymorphisms

INTRODUCTION

Both genetic and environmental factors are important in the development of systemic lupus erythematosus (SLE), a systemic autoimmune disease of unknown origin [1,2]. With respect to genetic background, deficiencies in components of the classical pathway of complements (C1q, C1r, C1s, C4 or C2) are known to be major predisposing risk factors for SLE [3–6]. In complement deficiencies, an abnormal clearance of not only immune complexes [3], but also apoptotic cells, has been suggested as contributive towards the occurrence of SLE [7]. Inappropriate levels of apoptotic nuclei are suggested to be a source of autoantigens in SLE [8].

Mannose-binding lectin (MBL) comprises a trimer of three identical polypeptides, and several trimers further combine to form a bouquet-like structure resembling C1q [9]. The MBL gene is located on the long arm of chromosome 10 at 10q11.2-q21 and contains 4 exons [10]. Several polymorphisms have been reported for the MBL gene, and a large interindividual difference in serum MBL concentration among test subjects is caused by the possession of variant alleles. Codon 52, 54 and 57 polymorphisms are all on exon 1, and the presence of any of the minority alleles results in a significant reduction of the serum MBL concentration. Furthermore, homozygosity for minority alleles results in almost complete deficiency of serum MBL [11,12]. This has been attributed to increased degradation of the mutated protein [12]. In the promoter region of the MBL gene, polymorphisms are reported at positions −550, −221 and + 4, and they also greatly influence the levels of serum MBL [13,14]. MBL mediates lectin-dependent activation of the complement pathway [9], and plays an important role in host defense against microorganisms by phagocytosis. Individuals lacking this protein could develop severe episodes of bacterial infections from early life [15–17].

Recently, several studies have suggested that MBL deficiency, or low serum MBL levels caused by polymorphisms in the structural portion or promoter region of the MBL gene, may be associated with occurrence of SLE [18–22]. Two possible explanations for the associations between MBL deficiency and the occurrence of SLE are suggested. Firstly, MBL can bind to and initiate uptake of apoptotic cells by macrophages [23], and an abnormal

Correspondence: Dr Akito Tsutsumi, 1-1-1 Tennodai, Tsukuba-city, Ibaraki 305–8575, Japan.
E-mail: atsutsum@md.tsukuba.ac.jp

clearance of apoptotic cells caused by MBL deficiency may result in the overexpression of autoantigens. Alternatively, viral infection is believed to be one of causes of SLE [24–26], and MBL deficiency may lead to more frequent infections. On the other hand, deposits of MBL were found in glomerular tissues of SLE patients [27,28], and D-mannose and N-acetylglycosamine, both possible ligands for MBL, are present in the salivary glands of patients with Sjögren's syndrome [29]. In this situation, MBL may have a pathogenic role during the course of SLE.

It has been reported that autoantibodies to C1q are associated with hypocomplementemia and glomerulonephritis [30]. If autoantibodies to MBL, a molecule similar to C1q in structure and functions, are present in patients with SLE, they may: reduce MBL levels; interfere with MBL functions; or bind to MBL deposited to various diseases. We investigated whether anti-MBL antibodies are indeed present in sera of Japanese patients with SLE.

PATIENTS AND METHODS

Patients and controls

Samples used for the study were taken from 111 Japanese patients with SLE, at Division of Rheumatology, Department of Internal Medicine, University Hospital of Tsukuba, Japan. All patients fulfilled the 1997 American College of Rheumatology (ACR) Classification Criteria for SLE. Patients with drug-induced lupus were excluded. The study was approved by the local ethics committee, and written informed consent was obtained from all participants of this study. Medical information including clinical manifestations, and laboratory data were collected simultaneously with sampling. Samples from 113 Japanese healthy volunteers served as controls.

Detection of immunoglobulin G (IgG) binding to MBL

Sumilon S plates (Sumitomo Bakelite, Tokyo Japan) were coated overnight at 4°C with 100 μl/well of recombinant MBL [31] in a carbonate/bicarbonate-buffer (pH 9·6) at a concentration of 1 μg/ml. The plates were washed three times with tris-buffered saline (TBS, pH 7·4) containing 0·05% Tween-20 (TBS/Tw). Unoccupied binding sites were blocked by incubation with 1% bovine serum albumin (BSA) in TBS for 1 h at 37°C. One hundred μl/well of serum samples diluted to 1 : 50 in TBS/Tw containing 0·3% BSA and 1 mM EDTA were added to the wells, and the plates were incubated overnight at 4°C. EDTA was included to inhibit the Ca^{2+} dependent binding of MBL to carbohydrates present on the Fc portion of IgG. All samples were analysed in triplicates. After incubation, 100 μl/well alkaline phosphate (AP)-conjugated goat antihuman IgG, specific for Fab fragment (Sigma, St Louis, MO, USA) diluted 1 : 5000 in TBS/Tw, was added to each well. The microtiter plates were incubated for 1 h at room temperature. Subsequently, alkaline phosphate substrate (Sigma) was added to each well. The plates were incubated for 2 h at room temperature. Optical densities (OD) were measured at 405 nm. The concentration of IgG reactive with MBL is expressed in units/ml of serum (U/ml), where the concentration in a standard sample was defined as 1000 U/ml. Standard curves were generated in all assays performed.

Inhibition assays

Anti-MBL positive sera diluted to 1 : 50 were preincubated with TBS or recombinant MBL at concentrations from 0·1563 μg/ml to 10 μg/ml at room temperature for 1 h. The samples were then put onto MBL-coated plates, and IgG binding to MBL was measured as described above.

Typing of the MBL gene

Genomic DNA was purified from peripheral blood leucocytes using the DnaQuick DNA purification kit (Dainippon Pharmaceuticals, Osaka, Japan), and stored at −30°C. Typing of the MBL gene allele was performed by using the polymerase chain reaction- restriction fragment length polymorphism method according to the methods of Madsen *et al.* [11]. The wild-type allele was designated as allele A, and codon 54 substitution (glycine to aspartic acid) was designated as allele B. Previous studies have shown that codon 52 and 57 polymorphisms are not present or extremely rare in the Japanese population [32,33].

Measurement of the serum MBL concentration by enzyme immunoassay

Serum concentration of MBL was measured by a specific enzyme immunoassay utilizing two rabbit polyclonal anti-MBL antibodies as described previously [31]. All samples were stored at −80°C and no previous freeze/thaw was done.

Statistics

Mann–Whitney *U*-test, Fisher's exact test, chi-square analysis and Spearman's rank correlation test were used. *P*-values of <0·05 were considered to be statistically significant.

RESULTS

Detection of autoantibodies to MBL in patients with SLE

Titers of IgG reactive with human MBL in patients with SLE were significantly higher than those in healthy controls; $P < 0{\cdot}0001$, median MBL concentration ± standard deviation (s.d.); 47·4 ± 49·3 and 30·6 ± 29·2, in SLE patients and healthy controls, respectively (Fig. 1). The assay was performed in the presence of EDTA in order to inhibit the binding between the carbohydrate recognition domain of MBL and carbohydrates on the Fc portion of IgG. Furthermore, selected samples were digested with pepsin and $F(ab')_2$ fragments were purified. $F(ab')_2$ fragments did bind to MBL coated plates, indicating that IgG–MBL interaction detected in this assay is indeed antigen-antibody binding (results not shown). We found a patient with an extremely high level of serum anti-MBL, and the titre of anti-MBL antibodies in the serum of this patient was designated 1000 U/ml. The number of subjects having a titre of more than 2 sd. above the average of healthy controls (89·5, indicated by dotted line in Fig. 1) was 9 of the patients with SLE, and 2 of the healthy controls. This difference was statistically significant ($P = 0{\cdot}0341$ by Fisher's exact test).

A titration curve could be adequately drawn using serial dilutions of the standard serum (Fig. 2a). In addition, adding excess amounts of recombinant MBL to diluted standard serum inhibited the binding of IgG to solid phase MBL in a dose dependent manner (Fig. 2b).

Associations between levels of anti-MBL antibodies, and MBL gene genotypes or serum concentrations of MBL in patients with SLE

Serum MBL concentrations reflected the MBL genotype of the individual in accordance with previous reports (Fig. 3) [11,12].

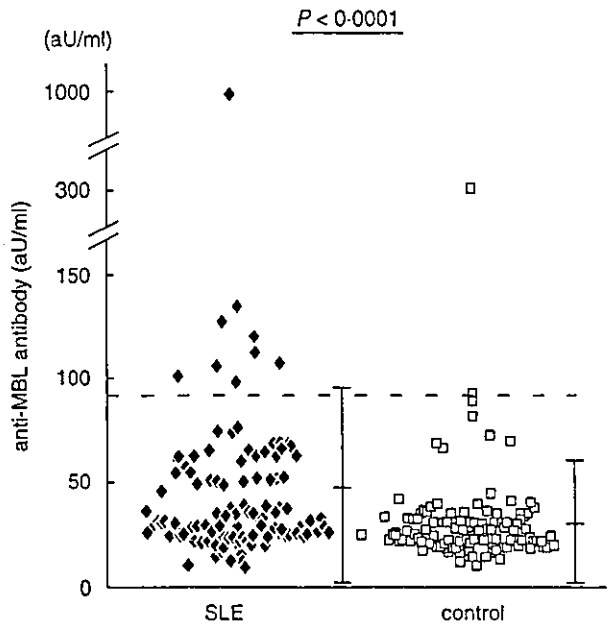

Fig. 1. Autoantibodies to mannose-binding lectin (MBL) in serum samples. Anti-MBL antibodies were measured in 111 samples from patients with systemic lupus erythematosus (SLE) and in 113 samples from healthy controls, in the presence of EDTA (1 mM). Dotted line indicates 2 standard deviation (s.d.) above average in healthy controls. *P*-value by Mann–Whitney *U*-test. aU, arbitrary units.

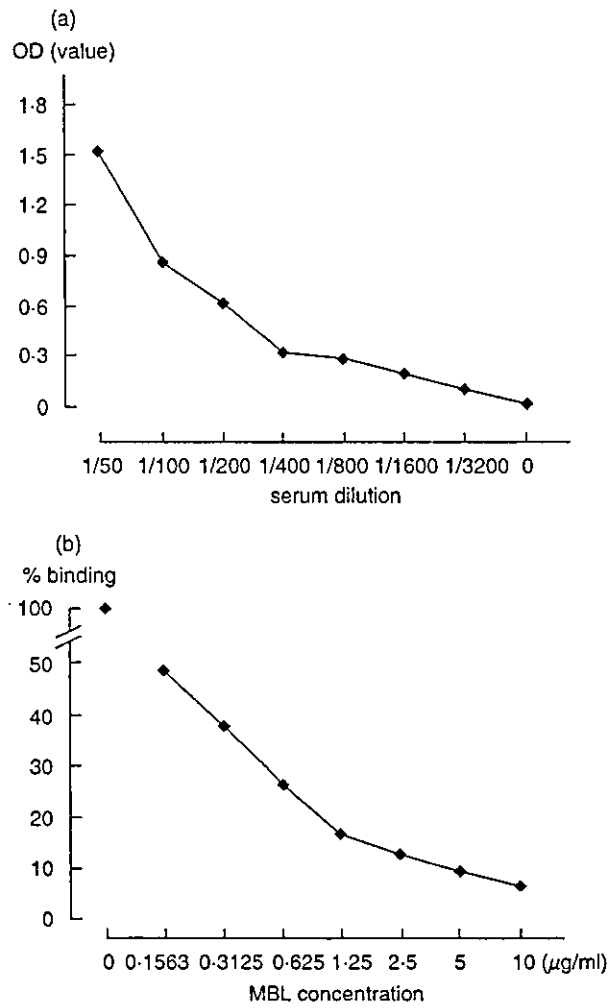

Fig. 2. Titration curve and inhibition assay for autoantibodies to mannose-binding lectin (MBL). (a) Titration curve for anti-MBL antibodies using serial dilutions of the standard serum in the presence of EDTA (1 mM). (b) Inhibition assay for anti MBL antibodies adding excess amount of recombinant MBL to diluted standard serum in the presence of EDTA (1 mM).

Serum MBL concentrations in SLE patients were not significantly different from those in healthy individuals ($P = 0{\cdot}5296$). Among individuals with the same genotype, SLE patients tended to have higher MBL concentrations than controls, but without statistical significance (AA; $P = 0{\cdot}3385$, AB; $P = 0{\cdot}5556$, BB; $P = 0{\cdot}1573$ by Mann–Whitney's *U*-test).

We next examined whether genotypes of the MBL gene in patients with SLE are associated with levels of anti-MBL antibodies (Fig. 4). Titres of anti-MBL antibodies tended to be lower in patients with allele B (AA; $60{\cdot}15 \pm 133{\cdot}3$, AB; $50{\cdot}10 \pm 26{\cdot}95$, BB; $38{\cdot}23 \pm 18{\cdot}88$), but no significant differences were observed.

Finally, we compared the serum concentrations of MBL and titres of anti-MBL antibodies in patients with SLE. We found no significant relationship between them (Fig. 5).

Relationships between the presence of anti-MBL antibodies in sera, and clinical characteristics or disease parameters of SLE

We investigated whether patients having anti-MBL antibodies at titres above 2 sd. of the average in healthy controls had some significant clinical characteristics (Table 1). No significant associations were observed. However, patients with higher serum concentration of anti-MBL antibodies tended to have a lower occurrence of anti-DNA antibodies, although statistical significance was not achieved. The incidence of infections requiring hospitalization during their course of SLE was not significantly higher in patients with higher serum concentration of anti-MBL antibodies.

We next analysed whether or not titres of anti-MBL antibodies are associated with various disease parameters of SLE in 111 SLE patients. Anti-DNA antibodies and total IgG tended to be positively related with anti-MBL antibodies, but statistical significance was not achieved. No other correlation was observed (Table 2).

DISCUSSION

In this study, we found the presence of autoantibodies against MBL in some patients with SLE. This is in accordance with the study by Seelen *et al.* [34], which was published very recently.

We confirmed that we were indeed detecting anti-MBL antibodies by; addition of EDTA in the enzyme immunoassay, thereby inhibiting the Ca^{2+} dependent binding of carbohydrate recognition domain on MBL to carbohydrates on IgG; digesting IgG with pepsin, and confirming that the binding region of IgG was on $F(ab')_2$; and detecting an inhibition of aqueous MBL to the binding of IgG to solid phase MBL. These methods and results are similar to those reported by Seelen *et al.* [34], except that we did detect dose dependent inhibition by our inhibition assay. The reason for this discrepancy is unclear, but may possibly be due to

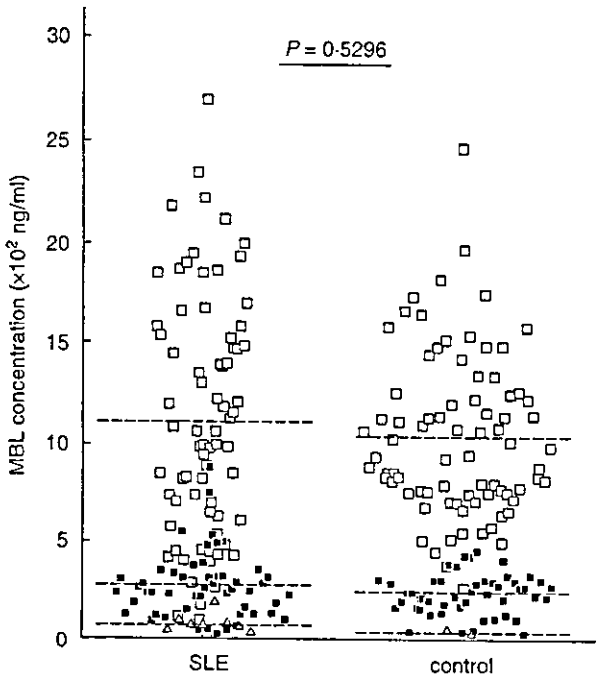

Fig. 3. Serum mannose-binding lectin (MBL) concentrations in 111 patients with systemic lupus erythematosus (SLE) and 113 healthy controls. Subjects with homozygosity for the codon 54 wild-type allele (□), subjects with heterozygosity for the codon 54 variant (■), and subjects with homozygosity for the codon 54 variant allele (Δ) are indicated in both patients with SLE and healthy controls. Dotted lines indicate average of titres of serum MBL concentrations in each genotype on both groups. *P*-value by Mann–Whitney *U*-test.

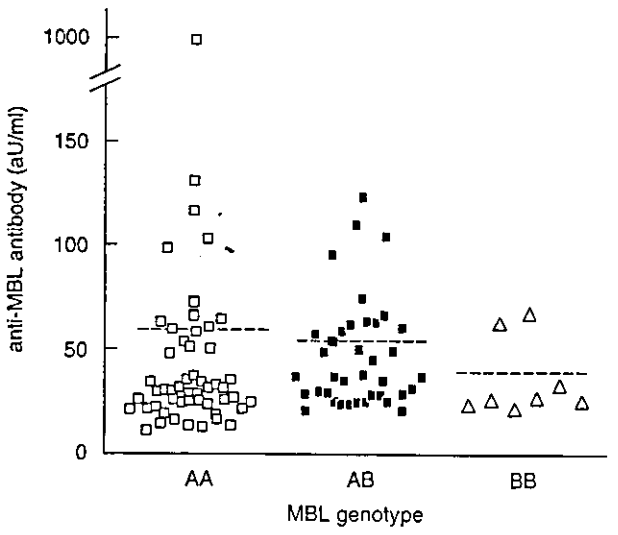

Fig. 4. Association between genotypes of the mannose-binding lectin (MBL) gene and levels of anti-MBL antibodies in patients with systemic lupus erythematosus (SLE). AA; homozygosity for the codon 54 wild-type allele, AB; heterozygosity for the codon 54 variant, BB; homozygosity for the codon 54 variant allele. Dotted lines indicate average of titres of anti-MBL antibodies in each genotype. aU, arbitrary units.

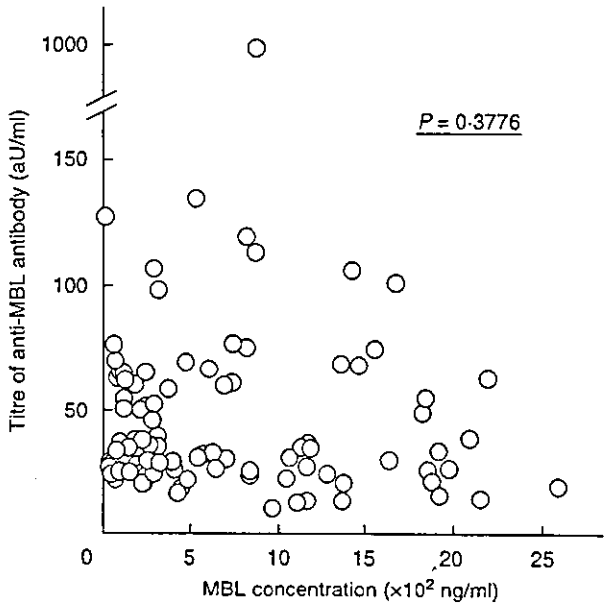

Fig. 5. Association between titres of anti mannose-binding lectin (MBL) antibodies and concentrations of MBL in systemic lupus erythematosus (SLE) patients. *P*-value by Spearman's rank correlation test. aU, arbitrary units.

Table 1. Discase characteristics of 111 patients with systemic lupus erythematosus (SLE) categorized by positivity of anti-mannose-binding lectin (MBL) antibody

	Positive (n = 9)	Negative (n = 102)	*P*-value
Malar rash	3	44	0·7309
Discoid lupus	0	13	0·5951
Photosensitivity	1	22	0·6821
Oral ulcers	2	20	0·9999
Arthritis	5	59	0·9999
Serositis	4	22	0·2099
Renal disorder	1	29	0·4399
Neurological disorder	0	9	0·9999
Haematologic disorder			
Haemolytic anemia	0	8	0·9999
leukopenia	4	52	0·7422
lymphopenia	4	48	0·9999
thrombocytopenia	1	27	0·4447
Anti-ds DNA Ab	4	74	0·1225
Anti-Sm Ab	0	8	0·9999
Antiphospholipid Ab	3	18	0·3673
ANA	8	95	0·5033
Infections requiring hospitalization	3	29	0·7155

Anti-MBL antibody positive was defined as having a titre higher than mean +2 s.d. of 113 healthy individuals. Serositis, pleuritis or pericarditis; renal disorder, proteinuria or cellular casts; neurological disorder, seizures or psychosis; Anti-ds DNA Ab, anti-double strand DNA antibody; Anti-Sm Ab, anti-Sm antibody; Antiphospholipid Ab, antiphospholipid antibody. *P* = AA + AB versus BB by chi-square analysis.

Table 2. Associations of titres of anti-mannose-binding lectin (MBL) antibody and various disease parameters of systemic lupus erythematosus (SLE) in 106 SLE patients

Disease parameters of SLE	*P*-value[a]
Anti-DNA antibody	0·2173
C3	0·8844
C4	0·2131
CH50	0·7919
IgG	0·0665
IgA	0·9026
IgM	0·1637

[a]Spearman's rank correlation test.

the nature of anti-MBL antibodies in individual patients, or concentrations or conformations of MBL used in the assays.

Similarities in structure and function exist between MBL and C1q, and it is known that C1q-deficient or anti-C1q antibody positive individuals have a high probability of developing SLE [5,30,35,36]. It has been reported that MBL deficiency may be associated with the occurrence of SLE [18–22], although deficiency of MBL is not an extremely high risk factor, in contrast to deficiencies of other complement molecules such as C1q. The presence of autoantibodies against MBL may cause similar pathological conditions to those found in MBL deficiency, as with the case of anti-C1q antibodies. In this context, it is noteworthy that a previous study has shown that anti-C1q antibodies do not recognize MBL [37], which suggests that anti-MBL and anti-C1q antibodies are not identical.

In accord to previous studies, serum MBL concentrations were closely associated with the MBL genotypes of the individuals studied (Fig. 3). However, in this study, no significant differences in serum MBL concentrations were observed between SLE patients and healthy controls, when individuals with the same genotype were compared. This is different from the study by Seelen *et al.* [34], where they found that serum MBL concentrations were higher in SLE patients than in controls. This difference may be due to differences in MBL genotype distributions or disease activities of SLE in the individuals studied, or other unknown factors.

We next asked whether there is any association between levels of anti-MBL antibodies and MBL genotypes. No such correlation was observed (Fig. 4). However, levels of anti-MBL antibodies in patients having genotype AB were higher than those in patients with genotype AA, if we excluded one patient with genotype AA with an extremely high level of anti-MBL antibodies (Fig. 4). In addition, some genotype BB patients had anti-MBL antibodies (Fig. 4). We went on to study the relationship between serum MBL concentration and levels of anti-MBL antibodies. There was no statistically significant relationship (Fig. 5). These findings support the notion that elevated serum MBL is not a causative factor for anti-MBL antibody production, and other factors should contribute to the production of these autoantibodies. One possible factor is the production of mutated MBL protein in genotype AB or BB individuals. Individuals with genotype AB or BB produce a mutated MBL protein which is degraded in sera, since they are unable to form a stable oligomerized structure [12,38]. These degraded MBL protein products may have a role in the occurrence of anti-MBL antibodies. However, at this point, this remains only a speculation. Other factors must be important as well, since some patients with genotype AA also have anti-MBL antibodies. Many questions need to be solved, before the mechanisms of autoantigen recognition and autoantibody production including anti-MBL antibodies could be clarified.

We examined the disease characteristics of SLE in anti-MBL antibodies positive patients (Table 1). There were no significant relationships between the possession of a significantly high titre of anti-MBL antibodies, and the characteristics or parameters of SLE. This is in accord with the report by Seelen *et al.* [34], which showed no difference between anti-MBL levels in sera of patients with active disease and inactive disease, especially concerning renal involvement. However, among patients having high titre of anti-MBL antibodies, smaller number of patients tended to have anti-DNA antibodies, and more patients (3 of 9 patients, 33%) developed intestinal pneumonitis, which usually occur in less than 10% of SLE patients [39]. Thus, we felt that some cases had somewhat atypical features of SLE. Whether this is only a coincidence or not is unclear. A study of larger number of patients should be done to clarify the clinical significance of anti-MBL antibodies in SLE.

It has been reported that individuals lacking MBL are prone to severe episodes of bacterial infections from early life [15–17]. A recent study has shown that presence of MBL minority alleles is a risk factor for infection in patients undergoing bone marrow transplantation [40]. It is also reported that the MBL deficiency, resulting from the possession of the variant alleles of the MBL gene, is a risk factor in patient receiving immunosuppressive therapy [19,20]. Although we anticipated that decreased MBL function caused by anti-MBL antibodies might lead to more frequent infections during the course of SLE, we could not find, in the present study, any significant associations between the presence of anti-MBL antibodies and the occurrence of infections requiring hospitalization after initiation of therapy of SLE. The effect of anti-MBL antibodies to increased susceptibility to infections in individuals under immunosuppressive therapy may not be as large as that caused by MBL gene polymorphisms. Since only 9 patients had significantly high titre of serum anti-MBL antibodies, a larger study is necessary to confirm this observation.

In conclusion, we detected anti-MBL antibodies in sera of patients with SLE. However, we could not find any significant relationships with MBL genotype, clinical characteristics and parameters of SLE in this study. Further studies are necessary to elucidate the actual functions of autoantibodies to MBL in the pathogenesis of SLE, and to determine the value of measuring these autoantibodies in clinical practice.

REFERENCES

1 Winchester RJ, Nunez-Roldan A. Some genetic aspects of systemic lupus erythematosus. Arthritis Rheum 1982; 25:833–7.
2 Deapen D, Escalante A, Weinrib L, Horwitz D, Bachman B, Roy-Burman P, Walker A, Mack TM. A revised estimate of twin concordance in systemic lupus erythematosus. Arthritis Rheum 1992; 35:311–8.
3 Atkinson JP. Complement deficiency: predisposing factor to autoimmune syndromes. Clin Exp Rheumatol 1989; 7:S95–101.
4 Arnett FC, Reveille JD. Genetics of systemic lupus erythematosus. Rheum Dis Clin North Am 1992; 18:865–92.
5 Bowness P, Davies KA, Norsworthy PJ, Athanassiou P, Taylor-Wiedeman J, Borysiewicz LK, Meyer PA, Walport MJ. Hereditary C1q deficiency and systemic lupus erythematosus. QJM 1994; 87:455–64.

6 Walport MJ. Complement deficiency and disease. Br J Rheumatol 1993; **32**:269–73.

7 Korb LC, Ahearn JM. C1q binds directly and specifically to surface blebs of apoptotic human keratinocytes. complement deficiency and systemic lupus erythematosus revisited. J Immunol 1997; **158**:4525–8.

8 Mevorach D, Zhou JL, Song X, Elkon KB. Systemic exposure to irradiated apoptotic cells induces autoantibody production. J Exp Med 1998; **188**:387–92.

9 Holmskov U, Malhotra R, Sim RB, Jensenius JC. Collectins: collagenous C-type lectins of the innate immune defense system. Immunol Today 1994; **15**:67–74.

10 Sastry K, Herman GA, Day L, Deignan E, Bruns G, Morton CC, Ezekowitz RA. The human mannose-binding protein gene. Exon structure reveals its evolutionary relationship to a human pulmonary surfactant gene and localization to chromosome 10. J Exp Med 1989; **170**:1175–89.

11 Madsen HO, Garred P, Kurtzhals JA, Lamm LU, Ryder LP, Thiel S, Svejgaard A. A new frequent allele is the missing link in the structural polymorphism of the human mannan-binding protein. Immunogenetics 1994; **40**:37–44.

12 Sumiya M, Super M, Tabona P, Levinsky RJ, Arai T, Turner MW, Summerfield JA. Molecular basis of opsonic defect in immunodeficient children. Lancet 1991; **29**:1569–70.

13 Madsen HO, Garred P, Thiel S, Kurtzhals JA, Lamm LU, Ryder LP, Svejgaard A. Interplay between promoter and structural gene variants control basal serum level of mannan-binding protein. J Immunol 1995; **15**:3013–20.

14 Madsen HO, Satz ML, Hogh B, Svejgaard A, Garred P. Different molecular events result in low protein levels of mannan-binding lectin in populations from southeast Africa and South America. J Immunol 1998; **161**:3169–75.

15 Koch A, Melbye M, Sorensen P *et al.* Acute respiratory tract infections and mannose-binding lectin insufficiency during early childhood. JAMA 2001; **285**:1316–21.

16 Summerfield JA, Ryder S, Sumiya M, Thursz M, Gorchein A, Monteil MA, Turner MW. Mannose binding protein gene mutations associated with unusual and severe infections in adults. Lancet 1995; **345**:886–9.

17 Summerfield JA, Sumiya M, Levin M, Turner MW. Association of mutations in mannose binding protein gene with childhood infection in consecutive hospital series. Br Med J 1997; **314**:1229–32.

18 Davies EJ, Snowden N, Hillarby MC, Carthy D, Grennan DM, Thomson W, Ollier WE. Mannose-binding protein gene polymorphism in systemic lupus erythematosus. Arthritis Rheum 1995; **38**:110–4.

19 Garred P, Madsen HO, Halberg P, Petersen J, Kronborg G, Svejgaard A, Andersen V, Jacobsen S. Mannose-binding lectin polymorphisms and susceptibility to infection in systemic lupus erythematosus. Arthritis Rheum 1999; **42**:2145–52.

20 Garred P, Voss A, Madsen HO, Junker P. Association of mannose-binding lectin gene variation with disease severity and infections in a population-based cohort of systemic lupus erythematosus patients. Genes Immun 2001; **2**:442–50.

21 Ip WK, Chan SY, Lau CS, Lau YL. Association of systemic lupus erythematosus with promoter polymorphisms of the mannose-binding lectin gene. Arthritis Rheum 1998; **41**:1663–8.

22 Tsutsumi A, Sasaki K, Wakamiya N *et al.* Mannose-binding lectin gene: polymorphisms in Japanese patients with systemic lupus erythematosus, rheumatoid arthritis and Sjögren's syndrome. Genes Immun 2001; **2**:99–104.

23 Ogden CA, deCathelineau A, Hoffmann PR, Bratton D, Ghebrehiwet B, Fadok VA, Henson PM. C1q and mannose binding lectin engagement of cell surface calreticulin and CD91 initiates macropinocytosis and uptake of apoptotic cells. J Exp Med 2001; **194**:781–95.

24 James JA, Kaufman KM, Farris AD, Taylor-Albert E, Lehman TJ, Harley JB. An increased prevalence of Epstein-Barr virus infection in young patients suggests a possible etiology for systemic lupus erythematosus. J Clin Invest 1997; **15** (100):3019–26.

25 James JA, Neas BR, Moser KL, Hall T, Bruner GR, Sestak AL, Harley JB. Systemic lupus erythematosus in adults is associated with previous Epstein-Barr virus exposure. Arthritis Rheum 2001; **44**:1122–6.

26 Okada M, Ogasawara H, Kaneko H *et al.* Role of DNA methylation in transcription of human endogenous retrovirus in the pathogenesis of systemic lupus erythematosus. J Rheumatol 2002; **29**:1678–82.

27 Hisano S, Matsushita M, Fujita T, Endo Y, Takebayashi S. Mesangial IgA2 deposits and lectin pathway-mediated complement activation in IgA glomerulonephritis. Am J Kidney Dis 2001; **38**:1082–8.

28 Lhotta K, Wurzner R, Konig P. Glomerular deposition of mannose-binding lectin in human glomerulonephritis. Nephrol Dial Transplant 1999; **14**:881–6.

29 Steinfeld S, Penaloza A, Ribai P *et al.* D-mannose and N-acetylglucosamine moieties and their respective binding sites in salivary glands of Sjögren's syndrome. J Rheumatol 1999; **26**:833–41.

30 Siegert C, Daha M, Westedt ML, van der Voort E, Breedveld F. IgG autoantibodies against C1q are correlated with nephritis, hypocomplementemia, and dsDNA antibodies in systemic lupus erythematosus. J Rheumatol 1991; **18**:230–4.

31 Ohtani K, Suzuki Y, Eda S *et al.* High-level and effective production of human mannan-binding lectin (MBL) in Chinese hamster ovary (CHO) cells. J Immunol Meth 1999; **222**:135–44.

32 Hakozaki Y, Yoshiba M, Sekiyama K *et al.* Mannose-binding lectin and the prognosis of fulminant hepatic failure caused by HBV infection. Liver 2002; **22**:29–34.

33 Sasaki K, Tsutsumi A, Wakamiya N, Ohtani K, Suzuki Y, Watanabe Y, Nakayama N, Koike T. Mannose-binding lectin polymorphisms in patients with hepatitis C virus infection. Scand J Gastroenterol 2000; **35**:960–5.

34 Seelen MA, Trouw LA, van der Hoorn JW, Fallaux-van den Houten FC, Huizinga TW, Daha MR, Roos A. Autoantibodies against mannose-binding lectin in systemic lupus erythematosus. Clin Exp Immunol 2003; **134**:335–43.

35 Slingsby JH, Norsworthy P, Pearce G, Vaishnaw AK, Issler H, Morley BJ, Walport MJ. Homozygous hereditary C1q deficiency and systemic lupus erythematosus. A new family and the molecular basis of C1q deficiency in three families. Arthritis Rheum 1996; **39**:663–70.

36 Walport MJ, Davies KA, Botto M. C1q and systemic lupus erythematosus. Immunobiology 1998; **199**:265–85.

37 Martensson U, Thiel S, Jensenius JC, Sjoholm AG. Human autoantibodies against Clq: lack of cross reactivity with the collectins mannan-binding protein, lung surfactant protein A and bovine conglutinin. Scand J Immunol 1996; **43**:314–20.

38 Garred P, Larsen F, Madsen HO, Koch C. Mannose-binding lectin deficiency – revisited. Mol Immunol 2003; **40**:73–84.

39 Eisenberg H, Dubois EL, Sherwin RP, Balchum OJ. Diffuse interstitial lung disease in systemic lupus erythematosus. Ann Intern Med 1973; **79**:37–45.

40 Rocha V, Franco RF, Porcher R *et al.* Host defense and inflammatory gene polymorphisms are associated with outcomes after HLA-identical sibling bone marrow transplantation. Blood 2002; **100**:3908–18.

Research article

The clinical implication and molecular mechanism of preferential IL-4 production by modified glycolipid-stimulated NKT cells

Shinji Oki, Asako Chiba, Takashi Yamamura, and Sachiko Miyake

Department of Immunology, National Institute of Neuroscience, National Center for Neuroscience and Psychiatry, Tokyo, Japan.

OCH, a sphingosine-truncated analog of α-galactosylceramide (αGC), is a potential therapeutic reagent for a variety of Th1-mediated autoimmune diseases through its selective induction of Th2 cytokines from natural killer T (NKT) cells. We demonstrate here that the NKT cell production of IFN-γ is more susceptible to the sphingosine length of glycolipid ligand than that of IL-4 and that the length of the sphingosine chain determines the duration of NKT cell stimulation by CD1d-associated glycolipids. Furthermore, IFN-γ production by NKT cells requires longer T cell receptor stimulation than is required for IL-4 production by NKT cells stimulated either with immobilized mAb to CD3 or with immobilized "αGC-loaded" CD1d molecules. Interestingly, transcription of *IFN-γ* but not that of *IL-4* was sensitive to cycloheximide treatment, indicating the intrinsic involvement of de novo protein synthesis for IFN-γ production by NKT cells. Finally, we determined *c-Rel* was preferentially transcribed in αGC-stimulated but not in OCH-stimulated NKT cells and was essential for IFN-γ production by activated NKT cells. Given the dominant immune regulation by the remarkable cytokine production of ligand-stimulated NKT cells in vivo, in comparison with that of (antigen-specific) T cells or NK cells, the current study confirms OCH as a likely therapeutic reagent for use against Th1-mediated autoimmune diseases and provides a novel clue for the design of drugs targeting NKT cells.

Introduction

Natural killer T (NKT) cells are a unique subset of T lymphocytes that coexpress the α/β T cell receptor (TCR) along with markers of the NK lineage such as NK1.1, CD122, and various Ly49 molecules. Most NKT cells express an invariant TCRα chain composed of Vα14-Jα281 segments in mice and Vα24-JαQ segments in humans associated with a restricted set of Vβ genes (1, 2). Unlike conventional T cells, which recognize peptides presented by MHC molecules, NKT cells recognize glycolipid antigens such as α-galactosylceramide (αGC) in the context of a nonpolymorphic MHC class I–like molecule, CD1d (3–5). After being stimulated by a ligand, NKT cells rapidly affect the functions of neighboring cell populations such as T cells, NK cells, B cells, and dendritic cells (6, 7). The various functions of NKT cells are mediated mainly by a rapid release of large amounts of cytokines, including IL-4 and IFN-γ. Whereas IFN-γ provides help for the Th1 responses required for defending against various pathogens and tumors, IL-4 controls the initiation of Th2 responses and has been shown to inhibit Th1-mediated autoimmune responses involved in experimental autoimmune encephalomyelitis (EAE), collagen-induced arthritis (CIA), and type 1 diabetes in NOD mice.

Given the exceptional ability of NKT cells to secrete regulatory cytokines in comparison with that of T cells or NK cells after primary stimulation, we have explored the possibility that ligand stimulation of NKT cells may lead to the suppression of Th1-mediated autoimmune diseases. We have previously demonstrated that OCH, a sphingosine-truncated analog of αGC, preferentially induces Th2 cytokines from NKT cells and that administration of OCH suppresses EAE and CIA by inducing a Th2 bias in autoantigen-reactive T cells (8, 9). However, the molecular mechanism accounting for the unique property of OCH to selectively induce IL-4 has not been clarified yet.

In this study, we used various stimuli, including the prototypic ligand αGC and its derivatives such as OCH, to investigate the molecular basis of the differential production of IL-4 and IFN-γ by NKT cells. We found that OCH, due to its truncated lipid chain, was less stable in binding the CD1d molecule than was αGC and exerted short-lived stimulation on NKT cells. IFN-γ production by NKT cells required longer TCR stimulation than was required for IL-4 production and de novo protein synthesis. *c-Rel* was preferentially transcribed in αGC-stimulated, but not in OCH-stimulated NKT cells and was shown to regulate IFN-γ production by NKT cells. Taken together, these results indicate that sustained TCR stimulation and concomitant c-Rel expression by αGC leads to the production of IFN-γ, whereas short-term activation and marginal *c-Rel* transcription by OCH results in preferential production of IL-4 by NKT cells.

Methods

Mice. C57BL/6 (B6) mice were purchased from CLEA Laboratory Animal Corp. (Tokyo, Japan). MHC class II–deficient I-$A^b\beta^{-/-}$ mice were purchased from Taconic (Germantown, New York, USA). All animals were kept under specific pathogen-free conditions and were used at 7–10 weeks of age. Animal care and use were in accordance with institutional guidelines.

Cell lines, antibodies, plasmids, and reagents. The NKT cell hybridoma (N38.2C12) (10) was a generous gift from K. Hayakawa (Fox Chase Cancer Center, Philadelphia, Pennsylvania, USA) and NS0-derived

Nonstandard abbreviations used: altered glycolipid ligand (AGL); altered peptide ligand (APL); CD28 responsive element (CD28RE); collagen-induced arthritis (CIA); c-Rel lacking C-terminal transactivation domain (c-RelΔTA); cycloheximide (CHX); cyclosporin A (CsA); experimental autoimmune encephalomyelitis (EAE); α-galactosylceramide (αGC); natural killer T (NKT); nuclear factor of activated T cell (NF-AT); phycoerythrin (PE); T cell receptor (TCR).

Conflict of interest: The authors have declared that no conflict of interest exists.

Citation for this article: *J. Clin. Invest.* 113:1631–1640 (2004). doi:10.1172/JCI200420862.

plasmacytoma cell lines expressing the Kb tail mutant of CD1d (11) were kindly provided by S. Joyce (Vanderbilt University, Nashville, Tennessee, USA). Cells were maintained in RPMI 1640 medium supplemented with 10% FCS, 2 mM L-glutamine, 100 U/ml penicillin/streptomycin, 2 mM sodium pyruvate, and 50 μM β-mercaptoethanol (complete medium). Phycoerythrin (PE)-labeled mAb to NK1.1 (PK136), peridinine chlorophyll protein/cyanine 5.5 –labeled mAb to CD3 (2C11), and recombinant soluble dimeric human CD1d:Ig fusion protein (DimerX I) were from BD PharMingen (San Diego, California, USA). For some experiments mAb's to NK1.1 (PK136) and CD3 (2C11) were conjugated with FITC. Polyclonal antibody to asialo GM_1 was purchased from WAKO Chemicals (Osaka, Japan). The pRc/CMV-c-Rel expression plasmid (12) was a generous gift from Grundström (Umeå University, Umeå, Sweden). The open reading frame of c-Rel cDNA was amplified by PCR and cloned into the retroviral pMIG(W) vector. The forward primer containing the *Xho*I recognition site was 5′-GACTCTCGAGATGGCCTCGAGTGGATATAA-3′ and the reverse primers used for wild-type c-Rel or the dominant negative mutant c-RelΔTA containing *Eco*RI recognition sites were 5′-GACTGAATTCTTATATTTTAAAAAAACCATATGTGAAGG-3′ and 5′-GACTGAATTCTTAACTCGAGATGGACCCGCATG-3′, respectively. The retroviral vector (pMIG) and packaging vector (pCL-Eco) were kindly provided by L. Van Parijs (Massachusetts Institute of Technology, Cambridge, Massachusetts, USA). Cyclosporin A (CsA) and cycloheximide (CHX) were from Sigma-Aldrich (St. Louis, Missouri, USA). All glycolipids were prepared as described in the Supplemental Methods (supplemental material available at http://www.jci.org/cgi/content/full/113/11/1631/DC1). The glycolipids were solubilized in DMSO (100 μg/ml) and were stored at -20°C until use.

Kinetic analysis of glycolipid stability on CD1d molecules. The kinetic analysis of glycolipid stability on CD1d molecules was performed as described previously with slight modifications (13). In brief, the NKT hybridoma was preincubated with 4 μM Fura red and 2 μM Fluo-4 (Molecular Probes, Eugene, Oregon, USA) at room temperature for 45 minutes, washed with RPMI 1640 medium containing 2% FCS (assay media), and resuspended in assay media. For determination of the optimal time for glycolipid loading onto $CD1d^+$ APCs, kinetic analysis was conducted using either αGC or OCH. According to the data obtained in Figure 2C, $CD1d^+$ APCs were pulsed with glycolipids (100 ng/ml) for 30 minutes. Then, cells were washed and resuspended in assay media. Glycolipid-pulsed APCs were harvested every 15 minutes after resuspension, mixed with NKT cells, and subjected to centrifugation in a table-top centrifuge (2,000 *g*) for 60 seconds. Cells were then resuspended briefly and analyzed for calcium influx into NKT hybridoma cells by flow cytometry (EPICS XL; Beckman Coulter, Tokyo, Japan). Activation was expressed as the percentage of Fura-red– and Fluo-4–stained cells in a high-FL1, low-FL4 gate.

In vivo glycolipid treatment and microarray analysis. Mice were injected intraperitoneally with 0.2 ml PBS containing 0.1 mg anti-asialo GM_1 Ab. Forty hours after injection, mice were injected intraperitoneally with αGC, OCH (100 μg/kg), or control vehicle in 0.2 ml PBS. After the indicated time point, liver mononuclear cells or spleen cells were harvested and NKT cells were purified with the AUTOMACS cell purification system using FITC-conjugated mAb to NK1.1 (PK136) and anti-FITC microbeads (Miltenyi Biotech GmbH, Bergisch Gladbach, Germany). The purity of NKT cells in the untreated samples and in the samples treated for 1.5 hours was more than 90%. The purity of the liver-derived samples and spleen-derived samples treated for 12 hours was more than 80% and 74%, respectively. Total RNA isolation with the RNeasy Mini Kit (Qiagen, Chatsworth, California, USA) and whole-microarray procedures using U74Av2 arrays (GeneChip System; Affymetrix, Santa Clara, California, USA) were done according to the manufacturers' instructions. From data image files, gene transcript levels were determined using algorithms in the Gene Chip Analysis Suit software (Affymetrix). Each probe was assigned a "call" of present (expressed) or absent (not expressed) using the Affymetrix decision matrix. Genes were considered to be differentially expressed when (a) expression changed at least threefold in the case of liver NKT-derived samples or twofold in the case of spleen NKT-derived samples compared with the expression in the negative control and (b) increased gene expression included at least one "present call."

In vitro stimulation. Liver mononuclear cells were isolated from B6 mice by Percoll density gradient centrifugation and were stained with PE-NK1.1 and FITC-CD3 mAb's. The $CD3^+NK1.1^+$ cells and $CD3^+NK1.1^-$ cells were sorted with an EPICS ALTRA Cell Sorting System (Beckman Coulter). The purity of the sorted cells was more than 95%. Sorted cells were suspended in RPMI 1640 medium supplemented with 50 μM 2-mercaptoethanol, 2 mM L-glutamine, 100 U/ml penicillin and streptomycin, and 10% FCS and were stimulated with immobilized mAb to CD3. Incorporation of [^{3}H]thymidine (1 μCi/well) for the final 16 hours of the culture was analyzed with a β-1205 counter (Pharmacia, Uppsala, Sweden). We measured the content of cytokines in the culture supernatants by ELISA. For quantitative PCR analysis, we harvested the cells after stimulation with glycolipid to prepare total RNA. Glycolipid stimulation of spleen cells in vitro was done similarly except that 1% syngeneic mouse serum was used instead of FCS. In some experiments, plates were coated with DimerX I (1 μg in 50 μl PBS per well) for 16 hours. After plates were washed extensively with PBS, glycolipids (100–200 ng in 50 μl PBS per well) were added, followed by incubation for another 24 hours. Then, NKT cells were added and cytokine production was analyzed after 72 hours of incubation.

Real-time PCR to monitor gene expression. Real-time PCR was conducted using a Light Cycler-FastStart DNA Master SYBR Green I kit (Roche Diagnostics GmbH, Mannheim, Germany) according to the manufacturer's specifications using 4 mM $MgCl_2$ and 1 pM primers. Values for each gene were normalized to those of a housekeeping gene (*GAPDH*) before the "fold change" was calculated (using crossing point values) to adjust for variations between different samples. Primers used for the analysis of gene expression are described in Supplemental Methods.

ELISA. For evaluation of cytokine production by NKT cells, sorted liver $CD3^+NK1.1^+$ NKT cells were stimulated with immobilized mAb to CD3 in complete medium. The level of cytokine production in cell culture supernatants or in serum was determined by standard sandwich ELISA using purified and biotinylated mAb sets and standards from BD PharMingen. After the addition of a substrate, the reaction was evaluated using a Microplate reader (BioRad).

Retroviral infection of NKT cells. The 293T cells were maintained in DMEM supplemented with 10% FCS, 2 mM L-glutamine, 100 U/ml penicillin/streptomycin, 2 mM sodium pyruvate, and 50 μM β-mercaptoethanol. Liver mononuclear cells were purified and cultured in complete medium supplemented with IL-2 (200 U/ml) for 24–48 hours. Cells were infected with retrovirus prepared by cotransfection of pMIG retroviral vector and pCL-Eco packaging vector into 293T cells. Cells were cultured in complete medium containing IL-2 and IL-15 (50 ng/ml) continuously for 3 days, and

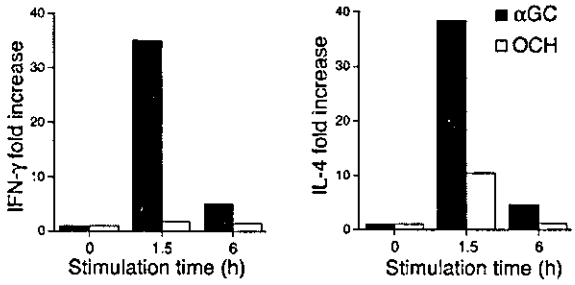

Figure 1
Transcriptional upregulation of cytokine genes by NKT cells stimulated with glycolipids in vivo. B6 mice were injected intraperitoneally with αGC or OCH (100 μg/kg), and liver NKT cells were isolated at the indicated time point. Total RNA was extracted and analyzed for cytokine mRNA by quantitative RT-PCR as described in Methods. Data are presented as "fold induction" of cytokine mRNA after glycolipid treatment. The amount of mRNA in NKT cells derived from untreated animals was defined as 1.

GFP-positive NKT cells were sorted and stimulated with immobilized mAb to CD3 for 48 hours. Culture supernatants were subjected to evaluation of cytokine production by ELISA.

Results

Preferential IL-4 production by OCH-stimulated NKT cells. The suppression of EAE by OCH was found to be associated with a Th2 bias of autoimmune T cells mediated by IL-4 produced by NKT cells (9). To confirm the primary involvement of NKT cells in the Th2 bias seen in the OCH treatment, we purified $CD3^+NK1.1^+$ NKT cells from B6 mice treated in vivo with αGC or OCH and measured the transcription of cytokine genes by quantitative RT-PCR. As shown in Figure 1, treatment with αGC greatly increased the expression of both IFN-γ and IL-4 at 1.5 hours after injection, whereas OCH induced a selective increase in IL-4 expression. When the IL-4/IFN-γ ratio was used for evaluating the Th1/Th2 balance, the NKT cells, isolated at 1.5 hours after injection of OCH were distinctly biased toward Th2 (Table 1). These results indicate that OCH is a selective inducer of rapid IL-4 production by NKT cells when administered in vivo.

Lipid chain length and cytokine production. Comparison of the structural difference between OCH and αGC (Figure 2A) raised the possibility that the lipid chain length of the glycolipid ligand may influence the cytokine profile of glycolipid-treated NKT cells. We compared αGC and OCH as well as newly synthesized analogs F-2/S-3 and F-2/S-7, which bear lipids of intermediate length (Figure 2A), for their ability to induce cytokine production by splenocytes. There was good correlation between the lipid tail length of each glycolipid and its ability to induce IFN-γ from the splenocytes, and a larger amount of IFN-γ was released into the supernatants after stimulation with the glycolipids with the longer sphingosine chain (Figure 2B, right). Regarding the ability to stimulate IL-4 production, the differences among OCH, F-2/S-3 and F-2/S-7 were less clear, as shown by IFN-γ induction. Similar results were obtained with liver mononuclear cells as responder cells (see Supplemental Figure 1). These results indicate that cytokine production by NKT cells, in particular IFN-γ production, is greatly influenced by lipid chain truncation of the glycolipid.

Differential half-life of NKT cell stimulation by CD1d-associated glycolipids. It is believed that the two lipid tails of the glycolipids (sphingosine base and fatty acyl chain) would be accommodated by the highly hydrophobic binding grooves of CD1d. To verify the hypothesis that the functional properties of each glycolipid may be determined by the stability of its binding to CD1d molecules, we evaluated the half-life of these glycolipids on CD1d molecules by estimating calcium influx into NKT hybridoma cells as described previously (13). To exclude the possible involvement of endosomal/lysosomal sorting in this assay, we used APCs expressing a CD1d mutant (Kb tail) that lacks the endosomal/lysosomal targeting signal (11). The cells express both β_2m and sCD1d1 fused to the transmembrane and cytosolic tail sequence of $H\text{-}2K^b$ at the carboxyl terminus and could bind to glycolipids such as αGC or OCH without their internalization and following endosomal/lysosomal sorting. Based on the kinetic analysis data for glycolipid loading efficiency shown in Figure 2C, we pulsed $CD1d^+$ APCs with glycolipids for 30 minutes.

Figure 2D shows that OCH was rapidly released from the CD1d molecule. A 30% reduction in calcium influx was observed after 15 minutes of incubation and only 25% of the initial amount of glycolipid remained after 60 minutes of incubation. In contrast, αGC was not released from CD1d molecule in the first 15 minutes and more than 50% of the initial amount of glycolipid remained after 60 minutes of incubation. F-2/S-3 and F-2/S-7 showed intermediate levels of release from CD1d molecule. These results support the idea that a glycolipid with a shorter sphingosine chain has a shorter half-life for NKT cell stimulation because of less-stable association with the CD1d molecule.

Kinetic analysis of cytokine production by activated NKT cells. Previous in vivo studies demonstrated that injection of αGC into B6 mice can induce a rapid and transient elevation of the serum IL-4 level and a delayed and persistent rise in IFN-γ (9, 14), suggesting that there is an intrinsic difference in kinetics for the production of IL-4 and IFN-γ by NKT cells. To address this issue further, we sorted $CD3^+NK1.1^+$ NKT cells, and conventional $CD3^+NK1.1^-$ T cells as a control, from liver lymphocytes and stimulated the sorted cells with immobilized mAb to CD3 for various periods of time. The cells were then incubated at rest without further stimulation and culture supernatants were harvested at 72 hours after initiation of the TCR stimulation. We found that TCR stimulation of NKT cells for as little as 2 hours could induce detectable IL-4 in the supernatant (Figure 3A, center). The amount of IL-4 in the supernatant rapidly increased in proportion to the duration of TCR stimulation (Figure 3A, center). In contrast, production of IFN-γ by NKT cells required at least 3 hours of TCR stimulation and gradually increased corresponding to the duration of TCR stimulation (Figure 3A, right). Conventional T cells required longer TCR stimulation for efficient cytokine production. We repeatedly confirmed that IFN-γ production by NKT cells required initial stimulation that was 1–2 hours longer and showed a slower accumulation than that of IL-4 production in this experimen-

Table 1
Transcriptional upregulation of cytokine genes by NKT cells stimulated with glycolipids in vivo

Stimulus	Time	*IFN-γ*	*IL-4*	Ratio (*IL-4/IFN-γ*)
αGC	1.5 h	35.0	38.3	1.09
	6 h	5.0	4.6	0.92
OCH	1.5 h	1.8	10.3	5.58
	6 h	1.5	1.1	0.72

The relative amounts of transcripts of *IFN-γ* and *IL-4* obtained from the experiment shown in Figure 1 are presented as "fold induction" relative to that of NKT cell–derived samples from untreated animals.

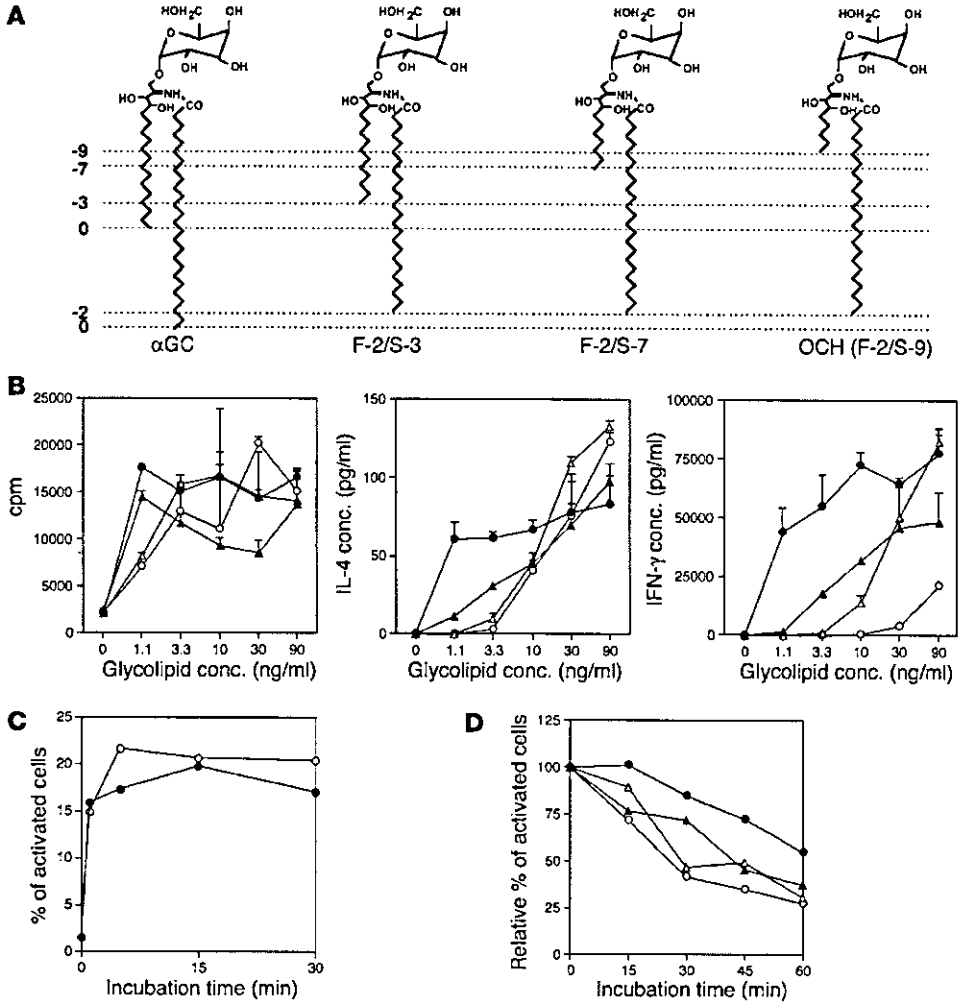

Figure 2

Differential properties of structurally distinct glycolipid derivatives. (**A**) Structures of αGC, OCH, and two other glycolipid ligands for NKT cells. F-2/S-3 has a truncation of two hydrocarbons in the fatty acyl chain (F) and of three hydrocarbons in the sphingosine chain (S) in comparison with αGC. OCH can be called F-2/S-9 accordingly. The numbers of truncated hydrocarbons in either lipid chain are shown along the left margin as negative integers. (**B**) Effect of αGC, OCH, and other glycolipids on proliferation and cytokine production of splenocytes. Splenocytes were stimulated with various concentrations (conc.) of αGC (filled circles), OCH (open circles), F-2/S-3 (filled triangles), or F-2/S-7 (open triangles) for 72 hours. Incorporation of [^{3}H]thymidine (1 μCi/well) during the final 16 hours of the culture was assessed (left), and IL-4 (center) or IFN-γ (right) in the supernatants was measured by ELISA. (**C**) Kinetic analysis of the loading of αGC (filled circles) or OCH (open circles) onto CD1d$^+$ APCs. See Methods for details. One experiment representative of two independent experiments with similar results is shown. (**D**) Calcium influx into NKT hybridoma cells after coculture with CD1d$^+$ APCs pulsed with αGC, OCH, F-2/S-3, or F-2/S-7. Data are presented as the activity remaining when the respective activity of glycolipid-loaded APCs for activation of the NKT cell hybridoma at time 0 was defined as 100%. Data are representative of three experiments with similar results.

tal setting. A similar kinetic difference was also observed when we used spleen-derived NKT cells (data not shown). These results indicate that NKT cells could produce IL-4 after a shorter period of TCR stimulation than is required for IFN-γ production.

To exclude the possibility that a qualitatively different CD1d complex with either αGC or OCH may bind with altered affinity to the TCR, we stimulated NKT cells with plate-bound αGC-CD1d complexes instead of mAb to CD3 for the periods of time indicated in Figure 3B. Consistent with the previous results obtained with anti-CD3 stimulation, the level of IL-4 in the culture supernatant was increased after shorter periods of incubation. In contrast, IFN-γ was efficiently produced after longer incubation, showing that the short pulse of NKT cells with plate-bound αGC-CD1d complexes could recapitulate the OCH phenotype. These results demonstrate that the timing of the CD1d-lipid interaction rather than the "shape" of the OCH-CD1d complex is the decisive factor in controlling polarization of cytokine production by NKT cells.

Differential transcriptional properties of cytokine genes. To clarify the molecular basis for different kinetics of cytokine production by activated NKT cells, we next examined the effects of CsA or CHX on the NKT cell responses. Without any inhibitors, IL-4 production was more rapid and had a higher rate than IFN-γ production (Figure 3C), confirming the kinetic difference required for induction of each cytokine shown in Figure 3A. Production of both IL-4

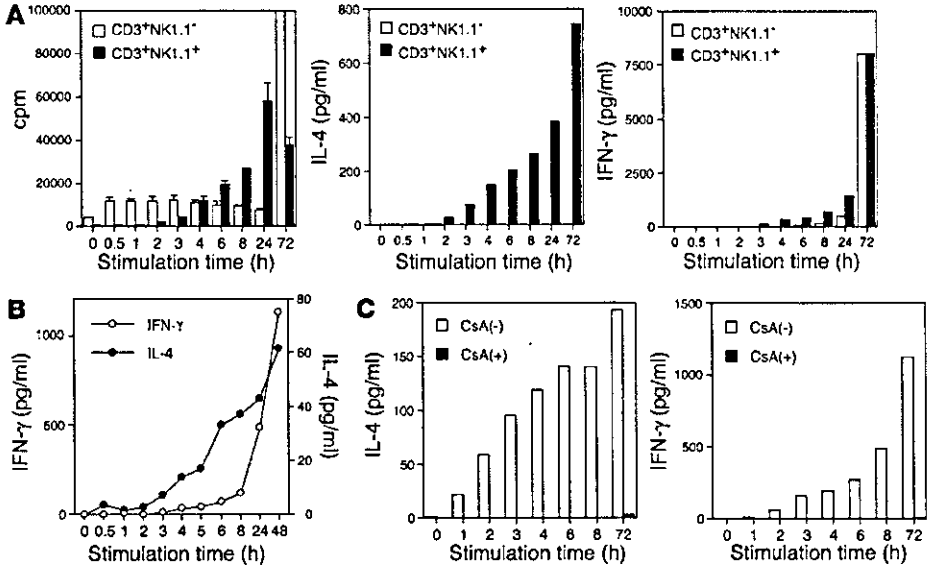

Figure 3

Kinetic analysis of NKT cell activation and cytokine production after glycolipid stimulation. (**A**) Differential production of IFN-γ and IL-4 by activated NKT cells. $CD3^+NK1.1^+$ NKT cells and conventional $CD3^+NK1.1^-$ T cells were purified from liver mononuclear cells by cell sorting. The sorted cells were stimulated with immobilized mAb to CD3 for the time indicated on the *x* axis and were then removed and recultured on a fresh culture plate without anti-CD3 stimulation for up to 72 hours from the start of the anti-CD3 stimulation. Incorporation of [^{3}H]thymidine (1 μCi/well) during the final 16 hours of the culture was assessed (left), and culture supernatants were analyzed for the production of IL-4 (center) and IFN-γ (right) by ELISA. One experiment representative of three independent experiments with similar results is shown. (**B**) NKT cells purified from liver mononuclear cells were stimulated with plates coated with DimerX I loaded with αGC and were analyzed as shown in **A**. (**C**) NKT cells purified from liver mononuclear cells were stimulated as shown in **A** in the presence [CsA(+)] or absence [CsA(–)] of CsA (1 μg/ml). Culture supernatants were analyzed for the production of IL-4 and IFN-γ by ELISA.

and IFN-γ after TCR stimulation, however, was almost completely inhibited by pretreatment of NKT cells with CsA.

Similarly, CsA abolished the transcriptional activation of *IL-4* and *IFN-γ* genes in activated NKT cells (Figure 4A), indicating that TCR signal–induced activation of nuclear factor of activated T cell (NF-AT) is indispensable for the production of both cytokines by NKT cells. Meanwhile, transcription of these cytokine genes showed different sensitivities to CHX treatment (Figure 4A). Although transcriptional activation of *IL-4* was barely affected by CHX treatment, transcription of *IFN-γ* gene was almost completely blocked after treatment with CHX. These results indicate that transcriptional activation of *IFN-γ*, but not that of *IL-4*, requires de novo protein synthesis.

Next, we analyzed the sensitivities of other cytokine genes to CsA and CHX treatment (15–17). As shown in Figure 4B, transcriptional activation of all cytokine genes tested was completely blocked by pretreatment of NKT cells with CsA. Interestingly, transcription of the *IL-2* gene and *GM-CSF* gene were blocked by CHX treatment. In contrast, transcriptional activation of *TNF-α* was resistant to CHX treatment. These results indicate that cytokines produced by NKT cells could be divided into two groups based on their dependence on de novo protein synthesis.

Selective c-Rel induction after stimulation with αGC. Although NKT cells secrete a large number of cytokines upon stimulation, the regulatory mechanisms for the expression of each cytokine are still poorly understood. The susceptibility of IFN-γ production to CHX indicates that some newly synthesized protein(s) would promote specific transcription of the *IFN-γ* gene in NKT cells. To identify the protein responsible for αGC-induced transcription of the *IFN-γ* gene, we purified NKT cells from glycolipid-administered I-$A^b\beta$-deficient mice, which have two- to threefold higher numbers of NKT cells in the liver and the spleen than do wild-type B6 mice (18), and assessed NKT cell–derived total RNA by microarray analysis. As shown in Table 2, a number of cytokines and chemokines were differentially expressed after in vivo treatment with either αGC or OCH. It is noteworthy, however, that significant induction of *IFN-γ* transcription was observed only in αGC-treated samples, not in OCH-treated samples. Overall, the data obtained correlated well with previous results showing that OCH is a selective inducer of IL-4 production from NKT cells (9). There was no transcriptional upregulation of cytokines genes such as the *IFN-γ* and *IL-4* genes 12 hours after treatment with either glycolipid, indicating that NKT cells have undergone quiescence at this time point in the context of transcriptional upregulation of cytokine genes, although some genes are still upregulated.

Through analyzing the microarray data, we identified the protooncogene *c-Rel*, a member of the NF-κB family of transcription factors, as a candidate molecule that may play a role in the *IFN-γ* transcription. As shown in Figure 5A, *c-Rel* was inducibly expressed in NKT cells 1.5 hours after stimulation with αGC. In contrast, OCH treatment did not induce *c-Rel* transcription (Figure 5A). The transcription of other NF-κB family genes such as *p65/RelA* and *RelB* was not upregulated after treatment with αGC or OCH. Real-time PCR analysis also confirmed the selective induction of *c-Rel* after αGC stimulation (Figure 5B). CsA treatment inhibited *c-Rel* transcription, but CHX did not (Figure 5C), indicating that the inducible transcription of c-Rel is directly controlled by TCR signal–mediated activation of the NF-AT (19).

It is already known that c-Rel serves as a pivotal transcription factor for the Th1 response that would directly induce IFN-γ production in conventional T cells (20). However, very little is known about the function of this protooncogene in NKT cells during TCR-mediated activation. We therefore conducted time course analysis for transcriptional activation of *c-Rel* in parallel with *IL-4* and *IFN-γ*. We stimulated NKT cells with immobilized mAb to CD3 for 30–100 minutes and then cultured them without further stimulation for a total of 120 minutes. As shown in Figure 5D, *IFN-γ* expression was slightly downregulated in the first 90 minutes of TCR stimulation and was significantly upregulated when the cells were stimulated for 100 minutes. Interestingly, we found that the kinetics of *c-Rel* transcription were similar to those of *IFN-γ* transcription (Figure 5D, right). In contrast, transcrip-

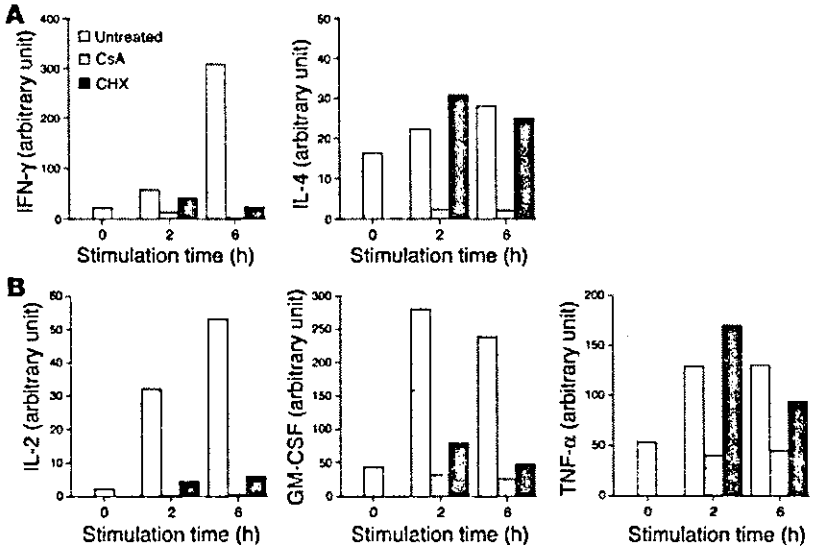

Figure 4
Differential sensitivity to CsA and CHX for transcriptional upregulation of *IFN-γ*, *IL-4*, and other cytokines. (**A**) Sorted NKT cells were pretreated with CsA (1 μg/ml) or with CHX (10 μg/ml) or without either reagent for 10 minutes and were then stimulated with immobilized mAb to CD3 for the indicated periods of time. Total RNA was extracted from each sample and analyzed for the relative amount of transcript of *IFN-γ* or *IL-4*. Data are presented as the amount of transcript in each sample relative to GAPDH. (**B**) Sorted NKT cells were pretreated with CsA (1 μg/ml) or with CHX (10 μg/ml) or without either reagent as shown in **A**. Total RNA was extracted from each sample and was analyzed for the relative amount of transcripts of *IL-2*, *GM-CSF*, or *TNF-α*. Data are presented as the relative amount of transcript in each sample.

tional activation of *IL-4* became evident 30 minutes after TCR stimulation and the transcript accumulated gradually in proportion to the duration of TCR stimulation. This result further confirmed that NKT cells require a longer TCR stimulus for IFN-γ expression.

Transcription of IFN-γ genes depends on c-Rel expression in NKT cells. To further investigate the functional involvement of c-Rel in the transcription of *IFN-γ* gene in NKT cells, we next examined whether forced expression of wild-type c-Rel or of its loss-of-function mutant could affect IFN-γ production by NKT cells. For this, we used bicistronic retroviral vectors expressing c-Rel along with GFP (pMIG/c-Rel) or a c-Rel dominant negative mutant that lacks the C-terminal transactivation domain but retains an intact Rel homology domain of c-Rel protein (pMIG/c-RelΔTA) (21) (Figure 6A). We infected liver-derived mononuclear cells with either retrovirus and stimulated sorted GFP-positive NKT cells with immobilized mAb to CD3 to analyze cytokine production. Retroviral transduction led to expression of GFP in approximately 10% of NKT cells (Figure 6B). Upon stimulation with mAb to CD3, GFP-positive cells from pMIG/c-Rel–infected cultures showed slightly augmented IFN-γ production compared with that of control pMIG-infected cells (Figure 6C). In contrast, GFP-positive cells from pMIG/c-RelΔTA–infected cultures secreted almost no IFN-γ after TCR stimulation (Figure 6C). These results demonstrate that inhibition of c-Rel function, via the introduction of a mutant form of c-Rel, abolishes IFN-γ production and that functional c-Rel is important for effective production of IFN-γ in activated NKT cells.

Discussion

In this study, we investigated the molecular mechanism for differential production of IFN-γ and IL-4 by activated NKT cells through a comparative analysis using the prototypic NKT cell ligands αGC and OCH. Treatment with αGC induced expression of both IFN-γ and IL-4 simultaneously, but OCH induced selective expression of IL-4 by NKT cells. Furthermore, we demonstrated that the CD1d-associated glycolipids with various lipid chain lengths showed different half-lives for NKT cell stimulation when applied in an endosome/lysosome-independent manner and induced the differential cytokine production by NKT cells in a lipid length–dependent manner. Accordingly, we demonstrated that IFN-γ production by NKT cells required longer TCR stimulation than did IL-4 production and depended on de novo protein synthesis. An NF-κB family transcription factor gene, the *c-Rel* gene, was inducibly transcribed in αGC-stimulated but not in OCH-stimulated NKT cells. Retroviral transduction of a loss-of-function mutant of c-Rel revealed the functional involvement of c-Rel in IFN-γ production by ligand-activated NKT cells. These results have provided a new interpretation of NKT cell activation — that the duration of TCR stimulation is critically influenced by the stability of each glycolipid ligand on CD1d molecules, which leads to the differential cytokine production by NKT cells.

We have previously demonstrated that administration of OCH consistently suppresses the development of EAE by inducing a Th2 bias in autoimmune T cells and that this Th2 shift is probably mediated by selective IL-4 production by NKT cells in vivo (9). Here we directly evaluated the cytokine profile of OCH-stimulated NKT cells using quantitative PCR analysis. Consistent with the previous assumption, NKT cells stimulated with OCH induced rapid production of IL-4 but led to only marginal induction of IFN-γ, confirming the presumed mechanism for the effect of OCH on EAE and CIA. As the "fold induction" of *IFN-γ* transcript after 1.5 hours of stimulation with αGC in microarray analysis was relatively low (fivefold for liver NKT cells and fourfold for spleen NKT cells) compared with the in vivo data, there are several possibilities to explain these results. First, quiescent transcripts of *IFN-γ* pre-existing in resting Vα14-invariant NKT cells (22) may raise the baseline of signal intensity in samples from untreated animals, resulting in a relative decrease in "fold induction" after glycolipid treatment. Second, detection of *IFN-γ* transcription in αGC-stimulated NKT cells might not be optimal, as injection of αGC induced a rapid elevation in IL-4 with the peak value at 2 hours and a delayed and prolonged elevation in IFN-γ in B6 mice (9). Third, αGC treatment significantly induces transcription of *CD154* (18.0-fold for αGC vs. 5.4-fold for OCH; data not shown), whose promoter has a functional NF-AT binding site and CD28 responsive element (CD28RE) (23, 24). Thus, augmented CD40/CD154 interaction may induce IL-12 expression by APCs, resulting in additional IFN-γ production (25). Finally, NKT cells are not necessarily the only source of IFN-γ after in vivo stimulation with αGC. The "serial" production of IFN-γ by NKT cells and NK cells has been demonstrated (6, 26). In particular, a C-glycoside analog of αGC has

Table 2
Differential gene expression patterns in αGC-treated and OCH-treated murine NKT cells

		Liver CD3+NK1.1+						Spleen CD3+NK1.1+					
		Untreated	αGC		OCH			Untreated	αGC		OCH		
Common name	GenBank		1.5 h	12 h	1.5 h	12 h			1.5 h	12 h	1.5 h	12 h	
IFN-γ	K00083	1.0 P	5.0 P	0.3 P	1.2 P	0.1 P		1.0 P	4.0 P	2.3 P	0.7 P	1.0 P	
IL-2	m16762	1.0 A	391.4 P	1.2 A	12.3 P	1.3 A		1.0 A	23.4 P	0.2 A	1.0 A	0.3 A	
IL-2	K02292	1.0 A	129.6 P	0.6 A	32.8 A	1.1 A		1.0 A	16.1 A	0.7 A	10.7 A	1.5 A	
GM-CSF	X03020	1.0 P	38.0 P	0.4 A	4.1 P	0.1 A		1.0 A	15.7 P	1.4 A	2.7 A	2.1 A	
IL-4	X03532	1.0 P	276.8 P	2.5 P	47.3 P	0.2 A		1.0 A	364.9 P	35.1 P	38.8 P	4.7 P	
IL-4	M25892	1.0 P	38.2 P	0.2 P	7.7 P	0.1 A		1.0 P	69.6 P	7.6 P	9.1 P	1.1 P	
IL-4	X03532	1.0 A	34.8 P	3.9 A	9.4 A	1.9 A		1.0 A	2.2 A	4.2 A	1.1 A	0.7 A	
IL-13	M23504	1.0 A	993.0 P	1.4 A	56.1 P	1.8 A		1.0 A	140.7 P	12.3 A	19.1 A	2.3 A	
TNF-α	D84196	1.0 P	30.8 P	2.1 P	1.7 P	1.2 P		1.0 P	16.5 P	2.5 P	1.8 P	2.6 P	
Lymphotoxin A	M16819	1.0 P	6.9 P	0.2 A	1.4 P	0.1 A		1.0 P	2.5 P	1.7 P	1.2 P	0.9 P	
IL-1α	M14639	1.0 P	25.1 P	5.6 P	3.1 P	4.4 P		1.0 P	6.7 P	5.8 P	1.1 P	2.7 P	
IL-1β	M15131	1.0 P	8.0 P	9.8 P	1.3 P	7.9 P		1.0 P	3.3 P	2.2 P	0.6 P	1.5 P	
*IL-1*RA	L32838	1.0 P	10.9 P	15.2 P	1.1 A	11.3 P		1.0 P	5.3 P	28.0 P	0.9 P	23.4 P	
IL-3	K01668	1.0 A	33.2 P	2.6 A	4.7 A	1.2 A		1.0 A	4.0 A	1.1 A	1.4 A	1.7 A	
IL-6	X54542	1.0 A	34.8 P	16.5 P	8.8 P	10.7 P		1.0 A	19.1 P	17.8 P	1.8 A	12.2 A	

Real-time PCR analyses were conducted for *IFN-γ* and *IL-4* as well as for other selected cytokine genes listed in Figure 4 (data not shown) to confirm the correlation with those obtained from microarray analysis. Each probe was assigned a "call" of present (P; expressed) or "absent" (A; not expressed) using the Affymetrix decision matrix. GenBank, GenBank accession number; *IL-1*RA, *IL-1* receptor antagonist.

recently been shown to induce Th1-type activity superior to that induced by αGC, and IL-12 is indispensable for the Th1-skewing effect of the analog (27), indicating the importance of IL-12 in augmenting IFN-γ production in vivo (14, 28). Interestingly, the C-glycoside analog induces production of IFN-γ and IL-4 by NKT cells less strongly than does αGC at 2 hours after in vivo administration. Given that αGC and C-glycoside analog have the same structure for their lipid tails, they might be expected to have comparable affinity for CD1d molecules, and the slightly "twirled" α-anomeric galactose moiety between C-glycoside and O-glycoside may modulate the agonistic effect of these glycolipids. Furthermore, the C-glycoside is more resistant to hydrolysis in vivo and may have an advantage for effective production of IL-12 by APCs. In fact, OCH induces marginal IL-12 production after in vivo administration (data not shown), which makes it unable to induce IFN-γ production by various cells. Therefore, the beneficial feature of OCH as an immunomodulator is that it does not trigger production of IFN-γ in vivo.

As described previously, NKT cells recognize glycolipid antigens in the context of the nonpolymorphic MHC class I-like molecule CD1d (4). Crystal structure analysis revealed that the mouse CD1d molecule has a narrow and deep binding groove with extremely hydrophobic pockets, A′ and F′ (29). Thus the two aliphatic hydrocarbon chains would be captured by this binding groove of CD1d and the more hydrophilic galactose moiety of αGC or OCH would be presented to TCR on NKT cells. As OCH is an analog of αGC with a truncated sphingosine chain, it could be predicted that truncation of the hydrocarbon chain would make it more unstable on CD1d, which might then affect the duration of TCR stimulation on NKT cells. We demonstrated in this study that OCH detached from the CD1d molecule more rapidly than did αGC after a short-term pulse in which the glycolipids were segregated from the endosomal/lysosomal pathway. Accordingly, we showed that the initiation of IFN-γ production by NKT cells required more prolonged TCR stimulation than was required for IL-4 production. Methods such as surface plasmon resonance were not appropriate for direct assessment of the interaction between glycolipids and CD1d, possibly because of unpredictable micelle formation and the poor solubility of glycolipids in aqueous solvents (30). The half-life of the interaction of glycolipids and CD1d was reported to be less than 1 minute by surface plasmon resonance (31), contradicting functional assays suggesting a much longer half-life. Therefore, we applied a biological assay to evaluate the stability of these glycolipids on CD1d molecules, as described previously (13).

The characteristics of OCH are somewhat analogous to those of an altered peptide ligand (APL) that has been shown to induce a subset of functional responses observed in intact peptide and, in some cases, induce production of selected cytokines by T cells (32–34). Thus, OCH and possibly other αGC derivatives could be called "altered glycolipid ligands" (AGLs). Although the biological effects of APLs and AGLs could mediate a series of similar molecular events in target cells, it should be noted that APLs and AGLs differ in their "conceptual features." That is, APLs are usually altered in their amino acid residues to modify their affinity for TCRs, whereas AGLs have truncation of their hydrocarbon chain responsible for CD1d anchoring. This paper has highlighted the duration of NKT cell stimulation by CD1d-associated glycolipids as being a critical factor for determining the nature of AGLs for selective induction of cytokine production by NKT cells.

Given that IL-4 secretion consistently precedes IFN-γ production by NKT cells after TCR ligation, we speculated there were critical differences in the upstream transcriptional requirements for the *IFN-γ* and *IL-4* genes in NKT cells. In support of this speculation, CHX treatment specifically inhibited the transcription of *IFN-γ* but not that of *IL-4*. In contrast, transcription of both cytokines was abolished by CsA treatment, indicating that TCR-mediated activation of NF-AT is essential for the production of both cytokines. TCR signal–induced NF-AT activation occurs promptly corresponding to calcium influx (35). Meanwhile, the protein expression of specific

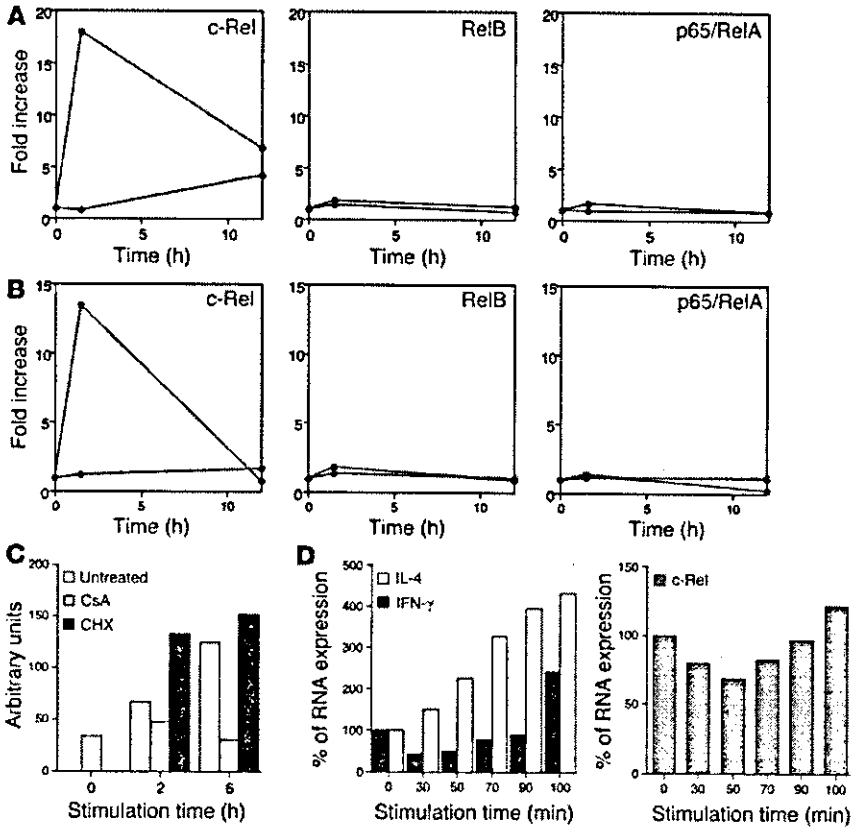

Figure 5
Induction of NF-κB family members in activated NKT cells. (**A**) Plotted values represent data of Affymetrix microarray analysis for the indicated genes.The αGC-stimulated (red lines) or OCH-stimulated (green lines) cells as well as unstimulated liver NKT cells were analyzed at the same time points and the data are presented as the relative value for stimulated NKT cells when the value in NKT cells derived from untreated animals was defined as 1. (**B**) Real-time PCR analysis for the same genes as in **A**. Data are presented as described in Figure 4. (**C**) Sorted liver NKT cells were pretreated with CsA or CHX and were stimulated with immobilized mAb to $CD3_\varepsilon$ and comparative values of c-Rel transcripts relative to GAPDH were determined. (**D**) Sorted liver NKT cells were stimulated with immobilized mAb to CD3 for the indicated periods of time and then were cultured without stimulation for up to a total of 120 minutes after the initial stimulation. Total RNA was extracted from each sample and analyzed for relative amounts of transcripts of *IFN-γ* or *IL-4* (left), or *c-Rel* (right). The amount of RNA derived from unstimulated NKT cells was defined as 100%.

transcription factors takes more time to accomplish. The requirement for prolonged TCR stimulation for initiation of *IFN-γ* transcription may be due to its dependency on specific gene expression.

Recently, Matsuda et al. have shown using cytokine reporter mice that Vα14-invariant NKT cells express cytokine transcripts in the resting state, but express protein only after stimulation (22). We obtained a similar result with our microarray analysis, in that many cytokine transcripts including *IFN-γ* and *IL-4* were detectable in unstimulated NKT cells derived from liver or spleen, because most of them were assigned a "call" of "present" by the Affymetrix decision matrix, which means they were significantly expressed. The mechanism of translation of pre-existing cytokine transcripts after activation of NKT cells remains to be investigated.

Through microarray analysis and real-time PCR, we next identified a member of the NF-κB family of transcription factors, c-Rel, as being a protein rapidly expressed after αGC treatment and possibly responsible for the transcription of *IFN-γ*. Treatment with αGC selectively upregulated *c-Rel* transcription 1.5 hours after stimulation of NKT cells in vivo. OCH treatment, however, showed no induction of *c-Rel* transcription. Although *c-Rel* is transcriptionally upregulated after TCR stimulation of T cells (36), transcription of other NF-κB family members such as *p65/RelA*, *RelB*, *NF-κB1*, and *NF-κB2* was unchanged (data not shown). CsA treatment inhibited c-Rel transcription, but CHX did not, indicating that inducible transcription of c-Rel was directly controlled by TCR signal–mediated activation of NF-AT, which is consistent with a previous report (19). Although the pre-existing NF-κB proteins in general provide a means of rapidly altering cellular responses by inducing the destruction of IκB in order to enable NF-κB to be free for nuclear translocation and DNA binding, most of the nuclear c-Rel induced after T cell stimulation has been shown to be derived from newly translated c-Rel proteins. In contrast, pre-existing c-Rel scarcely translocates to the nucleus at all (36), indicating that the nuclear induction of c-Rel in T lymphocyte requires ongoing protein synthesis. The retrovirally transduced loss-of-function mutant c-Rel (c-RelΔTA) significantly inhibited transcription of *IFN-γ* genes, indicating the crucial role of c-Rel in their transcription after activation of NKT cells. Although it is possible that the Rel domain of the dominant negative mutant may affect a number of NF-κB dimers, it is unlikely, because IFN-γ production by stimulated NKT cells were CHX sensitive and other NK-κB members were not induced after stimulation in the microarray analysis. Retroviral transduction of wild-type c-Rel into NKT cells resulted in slightly augmented expression of IFN-γ after stimulation. Induction of endogenous c-Rel after in vitro stimulation might reduce the effect of retrovirally introduced c-Rel protein.

Whereas c-Rel has been associated with the functions of various cell types, its role in the immune system was first demonstrated in its involvement in *IL-2* transcription (37), in which it possibly induced chromatin remodeling of the promoter (38). Recently, the promoters for the genes encoding *IL-3*, *IL-5*, *IL-6*, *TNF-α*, *GM-CSF*, and *IFN-γ* were shown to contain κB sites or the κB-related CD28RE. Gene targeting of *c-Rel* in mice revealed that *c-Rel*–deficient T cells have a defect in the production of IL-2, IL-3, IL-5, GM-CSF, TNF-α, and IFN-γ, although expression of some of the cytokines was rescued by the addition of exogenous IL-2 (39, 40). Regarding the involvement of c-Rel in IFN-γ production, the c-Rel inhibitor pentoxyfylline (41) selectively suppresses Th1 cytokine production and EAE induction (42), and transgenic mice expressing the *trans*-dominant form of IκBα have a defect in IFN-γ production and the Th1 response (43). Recently, an elegant study using *c-Rel*–deficient mice revealed *c-Rel* has crucial roles in IFN-γ production by activated T cells and conse-

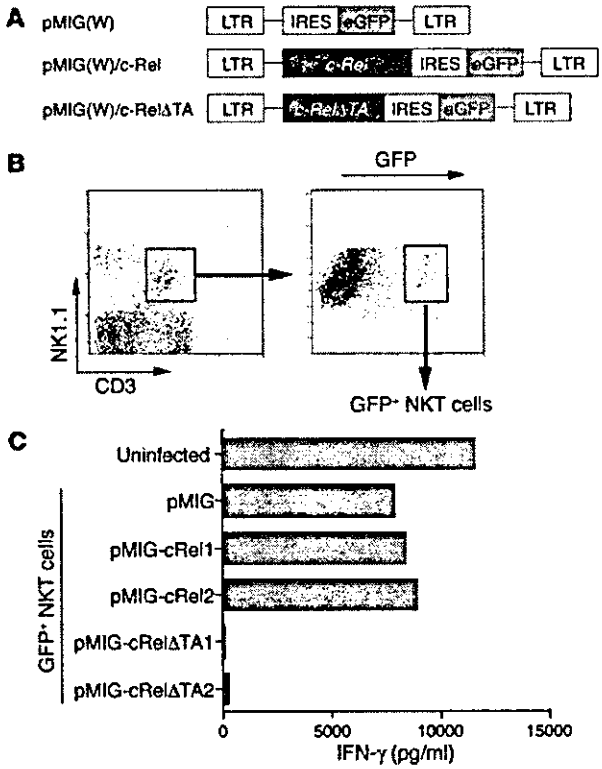

Figure 6
Cytokine production after retroviral transduction of c-Rel or c-RelΔTA into NKT cells. (**A**) DNA fragments encoding wild-type c-Rel or its mutant were cloned into the pMIG(W) bicistronic retrovirus vector. The mutant form of c-Rel (c-RelΔTA) lacks the transactivation domain of the c-Rel protein. LTR, long terminal repeat; IRES, internal ribosome entry site; eGFP, enhanced GFP. (**B**) Flow cytometric identification of cells transfected with the viral vector. Among the NK1.1+CD3+ liver NKT cells identified in the left panel, approximately 10% were GFP positive. The GFP-positive NKT cells were sorted for further analysis. (**C**) IFN-γ production by NKT cells transfected with c-Rel or its dominant negative mutant. The CD3+NK1.1+ NKT cells infected with the viruses were isolated based on their expression of GFP and were stimulated with immobilized mAb to CD3. For transduction of c-Rel or c-RelΔTA into NKT cells, two independent clones of each retroviral vector were used. The level of IFN-γ in the supernatants was measured by ELISA.

quent Th1 development by affecting the cellular functions of both T cells and APCs (20). Thus, the critical involvement of c-Rel for IFN-γ production in NKT cells is consistent with these findings.

Our results indicate that rapid calcium influx and subsequent NF-AT activation is essential for IFN-γ production by activated NKT cells and that c-Rel plays a crucial role in IFN-γ production as well. NF-AT shows quick and sensitive nucleocytoplasmic shuttling after TCR activation (35). Feske et al. demonstrated that the pattern of cytokine production by T cells was determined by the duration of nuclear residence of NF-AT (44) and that sustained NF-AT signaling promoted IFN-γ expression in CD4+ T cells (45). Considering the structural feature of αGC with longer lipid chain, sustained stimulation by αGC induces long-lasting calcium influx, resulting in sustained nuclear residence of NF-AT, and c-Rel protein synthesis, which enables NKT cells to produce IFN-γ. In contrast, the rather sporadic stimulation by OCH induces short-lived nuclear residence of NF-AT, followed by marginal c-Rel expression, which leaves NKT cells unable to produce IFN-γ (Figure 7). Thus, the kinetic and quantitative differences between αGC and OCH in the induction of transcription factors, such as NF-AT and c-Rel, determine the pattern of cytokine production by NKT cells. As CD1d molecules are nonpolymorphic and are remarkably well conserved among the species, the preferential induction of IL-4 production through NKT activa-

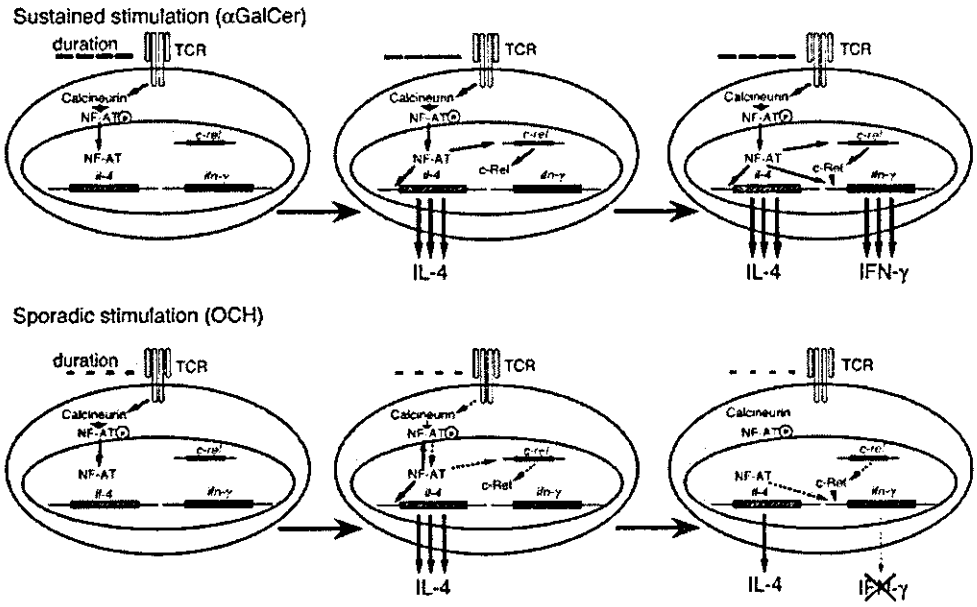

Figure 7
A model for the differential expression of IFN-γ and IL-4 after treatment of NKT cells with αGC or OCH. See text for details.

tion and subsequent Th2 polarization suggest that OCH may be an attractive therapeutic reagent to use for Th1-mediated autoimmune diseases such as multiple sclerosis and rheumatoid arthritis.

Acknowledgments

We thank Kyoko Hayakawa and Sebastian Joyce for providing the cell lines; Thomas Grundström for providing the c-Rel plasmid; and Luk Van Parijs for providing the retroviral vectors and packaging vector. We also thank Miho Mizuno and Chiharu Tomi for excellent technical assistance; and Yuki Kikai for cell sorting. We are grateful to John Ludvic Croxford for critical reading of the manuscript. This work was supported by the Organization for Pharmaceutical Safety and Research, Grant-in-Aid for Scientific Research (B) 14370169 from Japan Society for the Promotion of Science, Mochida Memorial Foundation, and Uehara Memorial Foundation.

Received for publication December 18, 2003, and accepted in revised form April 6, 2004.

Address correspondence to: Sachiko Miyake, Department of Immunology, National Institute of Neuroscience, NCNP, 4-1-1 Ogawahigashi, Kodaira, Tokyo 187-8502, Japan. Phone: 81-42-341-2711; Fax: 81-42-346-1753; E-mail: miyake@ncnp.go.jp.

1. Kronenberg, M., and Gapin, L. 2002. The unconventional lifestyle of NKT cells. *Nat. Rev. Immunol.* **2**:557-568.
2. Taniguchi, M., Harada, M., Kojo, S., Nakayama, T., and Wakao, H. 2003. The regulatory role of Vα14 NKT cells in innate and acquired immune response. *Annu. Rev. Immunol.* **21**:483-513.
3. Brossay, L., et al. 1998. CD1d-mediated recognition of an α-galactosylceramide by natural killer T cells is highly conserved through mammalian evolution. *J. Exp. Med.* **188**:1521-1528.
4. Kawano, T., et al. 1997. CD1d-restricted and TCR-mediated activation of Vα14 NKT cells by glycosylceramides. *Science.* **278**:1626-1629.
5. Spada, F.M., et al. 1998. CD1d-restricted recognition of synthetic glycolipid antigens by human natural killer T cells. *J. Exp. Med.* **188**:1529-1534.
6. Carnaud, C., et al. 1999. Cross-talk between cells of the innate immune system: NKT cells rapidly activate NK cells. *J. Immunol.* **163**:4647-4650.
7. Fujii, S.I., Shimizu, K., Smith, C., Bonifaz, L., and Steinman, R.M. 2003. Activation of natural killer T cells by α-galactosylceramide rapidly induces the full maturation of dendritic cells in vivo and thereby acts as an adjuvant for combined CD4 and CD8 T cell immunity to a coadministered protein. *J. Exp. Med.* **198**:267-279.
8. Chiba, A., et al. 2004. Suppression of collagen-induced arthritis by natural killer T cell activation with OCH, a sphingosine-truncated analog of α-galactosylceramide. *Arthritis Rheum.* **50**:305-313.
9. Miyamoto, K., Miyake, S., and Yamamura, T. 2001. A synthetic glycolipid prevents autoimmune encephalomyelitis by inducing TH2 bias of natural killer T cells. *Nature.* **413**:531-534.
10. Burdin, N., et al. 1998. Selective ability of mouse CD1 to present glycolipids: α-galactosylceramide specifically stimulates Vα 14+ NK T lymphocytes. *J. Immunol.* **161**:3271-3281.
11. De Silva, A.D., et al. 2002. Lipid protein interactions: the assembly of CD1d1 with cellular phospholipids occurs in the endoplasmic reticulum. *J. Immunol.* **168**:723-733.
12. Antonsson, A., Hughes, K., Edin, S., and Grundstrom, T. 2003. Regulation of c-Rel nuclear localization by binding of Ca2+/calmodulin. *Mol. Cell. Biol.* **23**:1418-1427.
13. Moody, D.B., et al. 2002. Lipid length controls antigen entry into endosomal and nonendosomal pathways for CD1b presentation. *Nat. Immunol.* **3**:435-442.
14. Fujii, S., Shimizu, K., Kronenberg, M., and Steinman, R.M. 2002. Prolonged IFN-γ-producing NKT response induced with α-galactosylceramide-loaded DCs. *Nat. Immunol.* **3**:867-874.
15. Akbari, O., et al. 2003. Essential role of NKT cells producing IL-4 and IL-13 in the development of allergen-induced airway hyperreactivity. *Nat. Med.* **31**:31.
16. Heller, F., Fuss, I.J., Nieuwenhuis, E.E., Blumberg, R.S., and Strober, W. 2002. Oxazolone colitis, a Th2 colitis model resembling ulcerative colitis, is mediated by IL-13-producing NK-T cells. *Immunity.* **17**:629-638.
17. Leite-de-Moraes, M.C., et al. 2002. Ligand-activated natural killer T lymphocytes promptly produce IL-3 and GM-CSF in vivo: relevance to peripheral myeloid recruitment. *Eur. J. Immunol.* **32**:1897-1904.
18. Chen, H., Huang, H., and Paul, W.E. 1997. NK1.1+ CD4+ T cells lose NK1.1 expression upon in vitro activation. *J. Immunol.* **158**:5112-5119.
19. Venkataraman, L., Burakoff, S.J., and Sen, R. 1995. FK506 inhibits antigen receptor-mediated induction of c-rel in B and T lymphoid cells. *J. Exp. Med.* **181**:1091-1099.
20. Hilliard, B.A., et al. 2002. Critical roles of c-Rel in autoimmune inflammation and helper T cell differentiation. *J. Clin. Invest.* **110**:843-850. doi:10.1172/JCI200215254.
21. Carrasco, D., et al. 1998. Multiple hemopoietic defects and lymphoid hyperplasia in mice lacking the transcriptional activation domain of the c-Rel protein. *J. Exp. Med.* **187**:973-984.
22. Matsuda, J.L., et al. 2003. Mouse Vα14i natural killer T cells are resistant to cytokine polarization in vivo. *Proc. Natl. Acad. Sci. U. S. A.* **100**:8395-8400.
23. Tsytsykova, A.V., Tsitsikov, E.N., and Geha, R.S. 1996. The CD40L promoter contains nuclear factor of activated T cells-binding motifs which require AP-1 binding for activation of transcription. *J. Biol. Chem.* **271**:3763-3770.
24. Parra, E., Mustelin, T., Dohlsten, M., and Mercola, D. 2001. Identification of a CD28 response element in the CD40 ligand promoter. *J. Immunol.* **166**:2437-2443.
25. Kitamura, H., et al. 1999. The natural killer T (NKT) cell ligand α-galactosylceramide demonstrates its immunopotentiating effect by inducing interleukin (IL)-12 production by dendritic cells and IL-12 receptor expression on NKT cells. *J. Exp. Med.* **189**:1121-1128.
26. Smyth, M.J., et al. 2002. Sequential production of interferon-γ by NK1.1+ T cells and natural killer cells is essential for the antimetastatic effect of α-galactosylceramide. *Blood.* **99**:1259-1266.
27. Schmieg, J., Yang, G., Franck, R.W., and Tsuji, M. 2003. Superior protection against malaria and melanoma metastases by a C-glycoside analogue of the natural killer T cell ligand α-galactosylceramide. *J. Exp. Med.* **198**:1631-1641.
28. Brigl, M., Bry, L., Kent, S.C., Gumperz, J.E., and Brenner, M.B. 2003. Mechanism of CD1d-restricted natural killer T cell activation during microbial infection. *Nat. Immunol.* **4**:1230-1237.
29. Zeng, Z., et al. 1997. Crystal structure of mouse CD1: An MHC-like fold with a large hydrophobic binding groove. *Science.* **277**:339-345.
30. Cantu, C., 3rd, Benlagha, K., Savage, P.B., Bendelac, A., and Teyton, L. 2003. The paradox of immune molecular recognition of α-galactosylceramide: low affinity, low specificity for CD1d, high affinity for αβ TCRs. *J. Immunol.* **170**:4673-4682.
31. Benlagha, K., Weiss, A., Beavis, A., Teyton, L., and Bendelac, A. 2000. In vivo identification of glycolipid antigen-specific T cells using fluorescent CD1d tetramers. *J. Exp. Med.* **191**:1895-1903.
32. Evavold, B.D., and Allen, P.M. 1991. Separation of IL-4 production from Th cell proliferation by an altered T cell receptor ligand. *Science.* **252**:1308-1310.
33. Chaturvedi, P., Yu, Q., Southwood, S., Sette, A., and Singh, B. 1996. Peptide analogs with different affinities for MHC alter the cytokine profile of T helper cells. *Int. Immunol.* **8**:745-755.
34. Boutin, Y., Leitenberg, D., Tao, X., and Bottomly, K. 1997. Distinct biochemical signals characterize agonist- and altered peptide ligand-induced differentiation of naive CD4+ T cells into Th1 and Th2 subsets. *J. Immunol.* **159**:5802-5809.
35. Zhu, J., and McKeon, F. 2000. Nucleocytoplasmic shuttling and the control of NF-AT signaling. *Cell. Mol. Life Sci.* **57**:411-420.
36. Venkataraman, L., Wang, W., and Sen, R. 1996. Differential regulation of c-Rel translocation in activated B and T cells. *J. Immunol.* **157**:1149-1155.
37. Ghosh, P., Tan, T.H., Rice, N.R., Sica, A., and Young, H.A. 1993. The interleukin 2 CD28-responsive complex contains at least three members of the NF κ B family: c-Rel, p50, and p65. *Proc. Natl. Acad. Sci. U. S. A.* **90**:1696-1700.
38. Rao, S., Gerondakis, S., Woltring, D., and Shannon, M.F. 2003. c-Rel Is required for chromatin remodeling across the IL-2 gene promoter. *J. Immunol.* **170**:3724-3731.
39. Gerondakis, S., et al. 1996. Rel-deficient T cells exhibit defects in production of interleukin 3 and granulocyte-macrophage colony-stimulating factor. *Proc. Natl. Acad. Sci. U. S. A.* **93**:3405-3409.
40. Kontgen, F., et al. 1995. Mice lacking the c-rel proto-oncogene exhibit defects in lymphocyte proliferation, humoral immunity, and interleukin-2 expression. *Genes Dev.* **9**:1965-1977.
41. Wang, W., Tam, W.F., Hughes, C.C., Rath, S., and Sen, R. 1997. c-Rel is a target of pentoxifylline-mediated inhibition of T lymphocyte activation. *Immunity.* **6**:165-174.
42. Rott, O., Cash, E., and Fleischer, B. 1993. Phosphodiesterase inhibitor pentoxifylline, a selective suppressor of T helper type 1- but not type 2-associated lymphokine production, prevents induction of experimental autoimmune encephalomyelitis in Lewis rats. *Eur. J. Immunol.* **23**:1745-1751.
43. Aronica, M.A., et al. 1999. Preferential role for NF-κ B/Rel signaling in the type 1 but not type 2 T cell-dependent immune response in vivo. *J. Immunol.* **163**:5116-5124.
44. Feske, S., Draeger, R., Peter, H.H., Eichmann, K., and Rao, A. 2000. The duration of nuclear residence of NFAT determines the pattern of cytokine expression in human SCID T cells. *J. Immunol.* **165**:297-305.
45. Porter, C.M., and Clipstone, N.A. 2002. Sustained NFAT signaling promotes a Th1-like pattern of gene expression in primary murine CD4+ T cells. *J. Immunol.* **168**:4936-4945.

International Immunology, Vol. 16, No. 3, pp. 423–431
doi: 10.1093/intimm/dxh046

Development of TCRB CDR3 length repertoire of human T lymphocytes

Junko Nishio[1], Mihoko Suzuki[1], Toshihiro Nanki[1], Nobuyuki Miyasaka[1] and Hitoshi Kohsaka[1]

[1]Department of Bioregulatory Medicine and Rheumatology, Graduate School, Tokyo Medical and Dental University, 1-5-45 Yushima, Bunkyo-ku, Tokyo 113-8519, Japan

Keywords: gene rearrangement, peripheral blood, thymus

Abstract

The third complementarity-determining region (CDR3) of TCR interacts directly with antigenic peptides bound to grooves of MHC molecules. Thus, it is the most critical TCR structure in launching acquired immunity and in determining fates of developing thymocytes. Since length is one of the components defining the CDR3 heterogeneity, the CDR3 length repertoires have been studied in various T cell subsets from humans in physiological and pathological conditions. However, how the CDR3 length repertoire develops has been addressed only by a few reports, including one showing that CDR3 of CD4 thymocytes becomes shorter during thymic development. Here, we explored multiple regulations on the development of the TCRB CDR3 length repertoires in the thymus and the peripheral blood. CDR3 length spectratyping was employed to examine thymocyte and peripheral T cell populations for their CDR3 length repertoires. We have found that repertoire distribution patterns depend on use of the BV gene. The BV-dependent patterns were shaped during thymic selections and maintained in the peripheral blood. Differences in the mean CDR3 length among different BV subsets were seen throughout lymphocyte development. We also observed that CDR3 was shortened in both CD4 and CD8 thymocytes. Of note, the degrees of the shortening depended on the CD4/CD8 lineage and on use of the BV gene. When expansions of peripheral T cell clones are negligible, no obvious difference was seen between mature thymocytes and peripheral lymphocytes. Thus, the TCRB CDR3 length repertoires are finely tuned in the thymus before the lymphocytes emigrate into the peripheral blood.

Introduction

Using surface receptors for antigens, αβ T cells recognize antigenic peptides bound to MHC class I or II molecules. Studies using X-ray crystallography have demonstrated that three-dimensional structures composed by the first, second and third complementarity-determining regions (CDR1, 2 and 3) of TCR α and β chains interact directly with peptides presented by the MHC molecules (1,2). Avidity of the interaction is defined by topological structure and location of charged amino acid residues of the interface peptides (3). In the TCR chain, CDR3 nucleic acid sequence is most diverse because it is generated by recombination of multiple V, D (in the case of TCRβ) and J gene segments, and by random addition of interlocating N region nucleotides (4,5). Since this region interacts most closely with the antigenic peptide, the diversity of the CDR3 amino acid sequences accounts for a wide array of antigen specificities within the functional T cell repertoire.

The molecular interaction of interface peptides is similarly important in association between antigenic peptides and MHC molecules. This interaction limits heterogeneity of peptides that can bind to the products of a given MHC allele (6). The length of the antigenic peptides is also restricted by interaction with MHC and with TCR (6). In contrast, the TCR CDR3 segments are more diverse in length. This might be explained by weaker association of antigenic peptides with TCR than with MHC (3,7). However, it remains to be seen how the CDR3 length repertoire is regulated during thymic development and in peripheral blood.

The αβ T cell repertoire develops through a number of selection steps in the thymus. TCRB gene rearrangement becomes complete first at the stage of $CD3^-CD4^+CD8^-$ immature single-positive (CD4 ISP) thymocytes (8,9). If their TCRB genes rearrange in-frame and their products pair successfully with pre-Tα chains, these cells survive and

Correspondence to: H. Kohsaka; E-mail: kohsaka.rheu@tmd.ac.jp

Transmitting editor: K. Yamamoto

Received 25 August 2003, *accepted* 25 November 2003

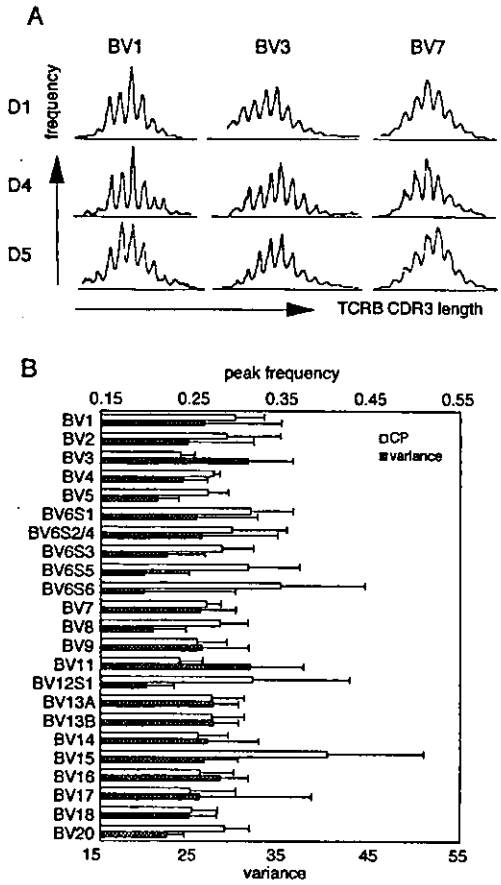

Fig. 1. BV-dependent differences in TCRB CLS histogram. (A) The histograms of the BV1, 3 and 7 subsets of peripheral CD4 T cells from three donors (D1, D4 and D5). (B) The CP frequencies and the variances in the individual BV subsets. They were calculated using TCRB CLS histograms of peripheral CD4 T cells from six child donors. The classification of the BV families was based on the definition by the WHO/International Union of Immunological Societies, Nomenclature Subcommittee on TCR Designation (30). The open columns and shaded columns represent the mean values of the CP frequencies and those of the variances respectively. The bars show their SD.

proliferate to become CD4+CD8+ double-positive thymocytes (8,10). They express TCRβ chains together with products of the in-frame rearranged TCRA gene. The double-positive thymocytes then undergo positive and negative selection, which make mature CD4 and CD8 T cell repertoires desirable to eliminate foreign pathogens. Although these processes are directed by the avidity of TCR with its ligand (11), their effects on the CDR3 length repertoire have hardly been explored.

The heterogeneity of the TCR CDR3 length in T cells at any developmental stages can be tested with TCR CDR3 length spectratyping (CLS). This method visualizes the distribution of TCR CDR3 length as histograms (12). It has been shown that typical histograms that are derived from mature peripheral T lymphocyte pools display a Gaussian-like distribution with 3-base spacing. If a histogram is biased by an unexpectedly high frequency at a specific length, it indicates that the studied population contains an expanded T cell clone whose CDR3 has the corresponding length. Based on this, the TCR CLS technique has been employed to study clonal perturbation of T cell repertoires from healthy donors and patients with various inflammatory diseases (13–19). The results have given us some insights into the physiology and pathology of T cell homeostasis.

The above facts all indicate the importance of discerning how heterogeneity of the CDR3 length repertoire is physiologically regulated, especially in the thymus. No gross difference in CDR3 length distribution between fetal and adult T cell pools has been reported (20). Yassai *et al.* (21) reported that thymocytes with shorter TCRB CDR3 are selected during transition from CD4+CD8+ thymocytes to CD4 SP thymocytes. Their subsequent report used murine systems to show that the shortening is mediated by TCR–peptide–MHC interaction in the thymus (22). Of note, they suggested that human repertoires might be under distinct regulation. Other investigators have described that different TCRB CDR3 lengths were preferred by different BV and BJ combinations in mice (23), and BJ genes in humans (24). However, no studies have addressed which stages in lymphocyte development are responsible for these differences.

How are the CDR3 length repertoires of various T cell subsets formed, modulated and maintained in the thymus and in the peripheral blood? How does the shortening occur in the human thymus? The present study was conducted to address these issues. By examining thymocytes and peripheral T cells for TCR CLS patterns, we have found that formation of human TCR CDR3 length repertoires is under multiplex regulations in the thymus.

Methods

Samples

Thymic fragments and peripheral blood were collected from child donors during heart surgery for correction of congenital cardiac anomalies. They were from 1 to 13 years old (mean 5.6 years old). They suffered from no immunological or hematological disorders. Consent forms were obtained before the operation. CD4 ISP thymocytes, mature CD4 and CD8 SP thymocytes, and peripheral CD4 and CD8 T lymphocytes were sorted from the thymic tissues or peripheral lymphocytes as described previously (25). Purities of the separated cells were >94%.

PCR

RNA were extracted from the sorted thymocytes and lymphocytes, and converted to cDNA (25). To amplify TCR transcripts with individual TCRBV family genes, the cDNA were subjected to PCR using a fluorescent TCRBC-specific anti-sense primer ($C_\beta b$) and a panel of sense oligonucleotide primers specific to TCRBV gene families (26). The amplification reaction consisted of 35 cycles of 1 min at 94°C, 1 min at 60°C and 1 min at 72°C, with final extension at 72°C for 7 min.

To amplify TCR transcripts with individual members of the BV7 family (BV7S1, BV7S2 and BV7S3 genes), a sense primer specific to the three BV7 family genes ($V_\beta 7os$: GGA GCT CAT

GTT TGT CTA CA) and a BC-specific antisense primer [$C_\beta a$ (26)] were used for primary PCR. The reaction consisted of 25 cycles of 1 min at 94°C, 1 min at 53°C and 1 min at 72°C followed by final extension at 72°C for 7 min. Part of the products were further amplified with a nested sense primer specific to BV7S1, BV7S2 or BV7S3 genes (V_β7S1s: TAC AGC TAT GAG AAA CTC TC; V_β7S2s: TAC AGT CTT GAA GAA CGG GT; or V_β7S3s: TCT ACA ACT TTA AAG AAC AGA C) and the fluorescent $C_\beta b$ primer. The reaction consisted of 25 cycles of 1 min at 94°C, 1 min at 53°C and 1 min at 72°C followed by final extension at 72°C for 7 min.

TCR CLS

The PCR products were fractionated on denaturing 7% polyacrylamide gel in a Hitachi SQ-5500 sequencer (Hitachi Electronics Engineering, Tokyo, Japan). The data were analyzed with the associated software to display histograms. Relative percentage of the TCRB transcripts of a given length to total TCRB transcripts in the BV subsets, which is called the frequency in this report, was calculated by dividing the fluorescence intensity of the corresponding peaks by the sum of the intensity of all peaks.

Statistical analyses

CDR3 length, defined as previously described (20), ranged from 6 to 60 bases. Nineteen frequency values within this range were treated as variables for cluster analyses, which were performed with Statistica 4.1J (Tulsa, OK). The variances were calculated as follows: $\sum_{n=2}^{20} F_{3n} \times (L_{3n} - \text{mean CDR3 length})^2$, where F_{3n} stands for the frequency value that corresponds to a given CDR3 length of L_{3n}. The Kruskal–Wallis test was used to compare the central peak (CP) frequencies, variances and mean CDR3 lengths of the histograms of different BV subsets. The Mann–Whitney test was used to compare these parameters of the histograms of the CD4 ISP thymocytes with those of the other populations.

Results

BV-dependent TCRB CDR3 length repertoires of peripheral CD4 T cells

In order to characterize unbiased TCRB CDR3 length repertoires of the mature T lymphocytes, peripheral CD4 T lymphocytes from six child donors were examined. This population was studied because biases of the T cell repertoires by clonally expanded T cells are more frequent in elder individuals and in the CD8 T cell pool (13,15,27,28). Although the histogram of each BV subset displayed a Gaussian-like distribution without outstanding biases, different BV subsets had slightly different patterns. Histograms of BV1, 3 and 7 gene families of three donors are shown to represent such differences (Fig. 1A). The shapes of different BV subsets were distinguished by the height of the CP that always had the highest frequency and by the width of the span. The histograms of BV1 had a high CP and narrow span, those of BV3 had a low CP and wide span, and BV7 had modestly high CP and a narrow span.

The characteristics were quantitatively assessed with the CP frequencies and the variances; the variances indicate span of the histograms. These two values were calculated for all BV subsets studied (Fig. 1B). Various combinations of CP frequencies and variances were observed. Reflecting the histogram pattern of the BV3 subset, its CP frequencies were low and the variances were remarkably large. This was also the case with the BV11 subset. The BV1 subset, as well as the BV6S1 subset, had high CP frequencies and small variances. The two parameters also describe the characteristics of the BV7 subset: moderate CP frequency and small variance.

Although some BV subsets had higher CP frequencies than BV1, or smaller variances than BV1 and 7, the BV1, 3 and 7 subsets were further studied to investigate how these differences develop during T lymphocyte development. The other BV subsets occasionally had minor and random biases, which should be due to small expansions of T cell clones. The characteristics of the three BV subsets and similarity within the same subsets could be illuminated by line graphs of the CDR3 length repertoires from six donors (Fig. 2A). Statistical comparison of the CP frequencies and the variances among the three subsets from six donors demonstrated that the CP frequencies of the BV1 subset were highest, while those of the BV3 subset were lowest, and that the variances in the BV3 subset were largest (Fig. 3A and B).

Pannetier *et al.* (23) reported that the mean TCRB CDR3 length of murine lymphocytes depends on use of BV genes. This was the case with human peripheral lymphocytes; the mean length of the TCRBV7 transcripts was longest, while that of the TCRBV3 transcripts was shortest (Fig. 3C).

Overall differences in the CLS patterns were elucidated by cluster analysis, which treated 19 frequency values at 6–60 bases as variables. A total of 18 histograms from six donors were segregated into three groups, each of which contained histograms of BV1, 3 or 7 subsets (Fig. 4A).

According to the published database, the BV7 family consists of BV7S1, 7S2 and 7S3 genes, while BV1 and 3 families have a single gene member (29). The histograms of the BV7 subset were derived from the PCR products that were generated with a primer specific to all BV7 family genes. In order to examine the TCR transcripts with individual BV7 genes, these transcripts were independently amplified with specific primers. The CLS distributions of the transcripts with the three BV7 genes were homologous and no statistical differences in CP frequency, variance or mean TCR length were observed (data not shown). Thus, the BV7 family subset was analyzed as a whole in the present studies.

Development of the BV-dependent repertoires in the thymus

TCRBV1, 3 and 7 transcripts that were derived from CD4 ISP thymocytes, and CD4 and CD8 SP thymocytes from the same set of donors were analyzed to study how the BV-dependent characteristics develop. As was discussed in our previous report (25), the CD4 ISP thymocytes have undergone TCRB gene rearrangement, but have not started positive or negative selection. Thus, unlike CD4 CD8 double-positive cells, a part of which are already under pressure of thymic selection, they are the best for investigation of primordial TCR repertoires.

The histograms of the CD4 and CD8 SP thymocytes shared the same characteristics as those of the peripheral CD4 cells